Journal of Statistical Physics, Vol. 90, Nos. 1/2, 1998

The Influence of Boundary Conditions on Solid-on-Solid Models

A. E. Patrick[1, 2]

Received July 23, 1996; final September 3, 1997

We investigate various 1D solid-on-solid (SOS) models using the transfer matrix method. The main results of the paper concern SOS interfaces near an attracting wall (line) when the end points of the interface are fixed away from the wall (line). We obtain typical interface shapes in the macroscopic scale. If attraction of the wall is strong enough, then a part of the interface is pinned to the wall (line) and the remaining parts of the interface form angles with the wall (line)—the contact angles. Explicit expressions for the contact angles are derived. We show also that for a certain range of parameters the models exhibit reentrant wetting and drying. As a result the free energy of the SOS model as a function of temperature can have up to three points of nonanalyticity. The fluctuations of the SOS interface are investigated in detail. Quite unusual fluctuations are observed at the contact points —the points where unpinned and pinned parts of the interface meet.

KEY WORDS: Contact angle; interface fluctuations; large deviations; reentrance; wetting.

1. INTRODUCTION

The present paper is devoted to a detailed investigation of several 1D Solid-On-Solid (SOS) models which invention is commonly attributed to Temperley, see Section 5 of ref. 12. The models are interesting as simplified models of various physical phenomena, such as phase separation in ferromagnets and binary liquids, or as a simplified model of polymer molecules.[13] In modern terminology, Temperley's original model is an SOS interface (no overhangs) with the state space of height variables $\mathbf{Z}^1$, and with only one end of the interface fixed. From the mathematical point of view the original model is next-to-trivial—equivalent to a 1D random

[1] Dublin Institute for Advanced Studies, School of Theoretical Physics, Dublin 4, Ireland.
[2] Dublin City University, School of Mathematical Sciences, Glasnevin, Dublin 9, Ireland.

0022-4715/98/0100-0389$15.00/0

walk. What was, however, quite non-trivial is that using his model Temperley succeeded in predicting the critical temperatures of various 2D Ising models. Another important feature of the SOS models was discovered much later—the interface fluctuations of 2D Ising models can be described qualitatively by the SOS interface.[4]

The model was not taken seriously by a wide audience at first (during the 60s and the 70s). However, the interest in the model rose significantly after a modification of the 2D Ising model that has a roughening transition below the Curie temperature was proposed and solved by Abraham,[1] and it was further shown that in the SOS limit the roughening transition persists. Subsequently, various SOS models were solved directly (that is, without prior solution of the corresponding Ising models), see refs. 5 and 6, and it was found that the SOS interfaces provide qualitatively correct description of the interfacial properties of 2D Ising models. Later on the SOS model was used in investigations of macroscopic properties of interfaces as a testing ground for various phenomenological theories, such as the Wulff construction and the Young equation, see refs. 7, 8, and 10, which further popularized the model.

So far, the most efficient, in our opinion, method for treating SOS models with two fixed ends (and, possibly, with some additional constraints) was based on an equivalence of ensembles, see ref. 10. This method, however, has two drawbacks. First, in its conventional form the equivalence of ensembles method allows one to obtain only the leading term in the asymptotic expansion of the free energy. Second, the predictions of microcanonical and canonical ensembles may be different for some observables (that is, the ensembles may simply not be equivalent at a certain level), then the method can not be applied at all. Fortunately in the case of SOS models it is possible to work directly in the microcanonical ensemble.

Although there already exists a rather large number of research and review articles devoted to SOS models a careful analysis of their probabilistic aspects is missing. In order to fill this gap several SOS models are analyzed from a unified point of view in the present paper. Some of the known results are rederived and new results are obtained using the transfer matrix method.

The paper is organized as follows. In Section 2 we consider the SOS interface with left and right ends fixed at $(0; L)$ and $(N; R)$, respectively. We derive there the leading term in the large N asymptotic expansion for the partition function, the distribution of fluctuations of height variables around their mean values, and the joint distribution of an arbitrary pair of height variables, see Eqs. (2.6) and (2.17).

Section 3, where we study the SOS interface near an attracting wall, is the central part of the paper. Employing the transfer matrix technique we

obtain an integral representation for the partition function of the model, see Eqs. (3.11) and (3.12), and calculate the large N asymptotic expansions for the partition function, see Eqs. (3.13), (3.15), (3.16), and (3.20). In Section 3.4 we use the integral representation of the partition function to find the typical (macroscopic) shape of the SOS interface that has its end points fixed above the attracting wall, see Eq. (3.35). If the attraction of the wall is strong enough then a part of the interface is pinned to the wall while the remaining parts of the interface form an angle with the wall—the contact angle. The explicit expression for the contact angle is given by Eq. (3.14). The distributions of fluctuations of the pinned and unpinned parts of the interface, see Eqs. (3.39) and (3.40), are derived in much the same way as the distributions in Section 2. What needs significantly more effort and yields quite a non-trivial result, see Eq. (3.46), is the investigation of fluctuations near the contact points—the points where pinned and unpinned parts of the interface meet.

Section 4 is devoted to an investigation of the SOS interface in the presence of a pinning line (no walls). Using the transfer operator we obtain integral representations of the partition function, see Eqs. (4.3) and (4.4). Then we derive the typical (macroscopic) shapes of the interface, see Eqs. (4.11) and (4.12), explicit expression for the contact angle, see Eq. (4.5), and the distribution of fluctuations of the unpinned and pinned parts of the interface and of the contact points. One of the striking distinctive features of the interface in the absence of the wall is that the corresponding contact angles are independent of the parameter J.

In Section 5 we discuss the results obtained in Sections 2–4. In particular, we claim there that the SOS interface has a cusp at contact points in all scales (except microscopic, where the interface is "shapeless"). Contrary to the beliefs present in physics literature rounding of the cusp does not take place in any scale.

Note on terminology: When describing an expression like

$$aN^{\gamma}e^{Nr(x)}$$

we call a—the amplitude, γ—the exponent, and $r(x)$—the rate function.

2. SOS MODEL WITH INTEGER HEIGHTS

The state space of the height variables in this version of the SOS model is $\mathbf{Z}^1$. The joint distribution of the sequence of height variables $\boldsymbol{h}_{N-1} \equiv \{h_j\}_{j=1}^{N-1}$ is given by

$$\mathbf{P}(\boldsymbol{h}_{N-1}) = Z_{N,L,R}^{-1} \exp\left[-\beta J \sum_{j=1}^{N} |h_j - h_{j-1}| \right] \tag{2.1}$$

where $h_j \in \mathbf{Z}^1$, $j=0, 1,..., N$; and $h_0 = L$, $h_N = R$ (the boundary conditions). The partition function $Z_{N,L,R}$ is given by

$$Z_{N,L,R} = \sum_{h_1,...,h_N=-\infty}^{\infty} e^{-\beta J|h_1 - L|} \sum_{j=2}^{N} e^{-\beta J|h_j - h_{j-1}|} \delta(h_N; R) \tag{2.2}$$

where $\delta(h_N; R)$ is the Kronecker symbol (that is, $\delta(k; l) = 1$ if $k = l$, and $\delta(k; l) = 0$ if $k \neq l$, for any integer k, l).

Using the integral representation

$$\delta(k; l) = \frac{1}{2\pi} \int_{-\pi}^{\pi} d\omega \, e^{i\omega(k-l)} \tag{2.3}$$

one can perform the summation over $h_1,..., h_N$ consecutively

$$\begin{aligned} Z_{N,L,R} &= \frac{1}{2\pi} \int_{-\pi}^{\pi} d\omega \, e^{-i\omega R} \sum_{h_1,...,h_N} \prod_{j=1}^{N} e^{-\beta J|h_j - h_{j-1}|} e^{i\omega h_N} \\ &= \frac{1}{2\pi} \int_{-\pi}^{\pi} d\omega \, e^{i\omega(L-R)} \Lambda^N(\omega) \end{aligned} \tag{2.4}$$

where

$$\Lambda(\omega) = \sum_{h=-\infty}^{+\infty} e^{-\beta J|h| + i\omega h} = \frac{\sinh \beta J}{\cosh \beta J - \cos \omega} \tag{2.5}$$

The large N asymptotic expansion for the remaining integral over ω can be found using the steepest descent method, see ref. 11. For the (most commonly used) boundary conditions $L = [lN]$, $R = [rN]$, (where $[x]$ denotes the integer part of x) we obtain

$$Z_{N,L,R} = \frac{\Lambda^N(\omega_*) \, e^{i\omega_*(L-R)}}{\sqrt{-2\pi N \Phi''(\omega_*)}} [1 + O(N^{-1})] \tag{2.6}$$

where $\omega_* = ig(l-r)$,

$$g(x) = -\log\left[\frac{\sqrt{1 + x^2 \sinh^2 \beta J}}{1-x} - \frac{x}{1-x} \cosh \beta J \right] \tag{2.7}$$

and

$$\Phi''(\omega_*) = \frac{d^2}{d\omega^2} \log \Lambda(\omega) \Big|_{\omega=\omega_*} = -\frac{\cosh g(l-r)}{\cosh \beta J - \cosh g(l-r)} - (l-r)^2 \tag{2.8}$$

The main properties of the function $g(l-r)$ are summarized in the following lemma, which proofs can be found in ref. 11.

Lemma 2.1. The function $g(x)$ is an increasing, infinitely differentiable, and odd function on $(-\infty; \infty)$.

Using Eq. (2.6) we conclude that the free energy per degree of freedom $f_\beta(l-r)$ is given by

$$-\beta f_\beta(l-r) = \lim_{N\to\infty} \frac{1}{N} \log Z_{N,L,R} = \log \Lambda(\omega_*) - (l-r)\, g(l-r) \quad (2.9)$$

2.1. The Distribution of Height Variables

To calculate the distributions of the random variables h_X note that

$$\Pr[h_X = Y] = \frac{Z_{X,L,Y} Z_{N-X,Y,R}}{Z_{N,L,R}} \quad (2.10)$$

Let $L=[lN]$, $R=[rN]$, $X=[\gamma N]$, and $Y=\chi N+\tau\sqrt{N}+o(\sqrt{N})$ (more complicated dependence of L, R, and X on N requires only minor technical modifications). Then using the steepest descent method, see ref. 11, one obtains

$$Z_{X,L,Y} = \frac{\Lambda^X[\omega_1^*(\chi)]\, e^{i\omega_1^*(\chi)[L-Y]}}{\sqrt{-2\pi X \Phi''[\omega_1^*(\chi)]}} \left[\exp\left\{ \frac{\tau^2}{2\gamma\Phi''[\omega_1^*(\chi)]} \right\} + O(N^{-1/2}) \right] \quad (2.11)$$

$$Z_{N-X,Y,R} = \frac{\Lambda^{N-X}[\omega_2^*(\chi)]\, e^{i\omega_2^*(\chi)[Y-R]}}{\sqrt{-2\pi(N-X)\,\Phi''[\omega_2^*(\chi)]}} \times \left[\exp\left\{ \frac{\tau^2}{2(1-\gamma)\,\Phi''[\omega_2^*(\chi)]} \right\} + O(N^{-1/2}) \right]$$

where $\omega_1^*(\chi) = ig[(l-\chi)/\gamma]$ and $\omega_2^*(\chi) = ig[(\chi-r)/(1-\gamma)]$.

In the next lemma we find the concentrating value for $h_{[\gamma N]}/N$, that is, the maximum point χ_γ^* of the rate function

$$\mathscr{R}_\gamma(\chi) = i\omega_1^*(\chi)[l-\chi] + \gamma \log \Lambda[\omega_1^*(\chi)] + i\omega_2^*(\chi)[\chi-r] + (1-\gamma)\log \Lambda[\omega_2^*(\chi)] \quad (2.12)$$

of the product $Z_{X,L,Y}Z_{N-X,Y,R}$. We also show that the (infinitely differentiable) function $\mathscr{R}_\gamma(\chi)$ is strictly concave, therefore, the distribution of $h_{[\gamma N]}/N$ indeed concentrates around χ_γ^* as $N \to \infty$. Having found χ_γ^* we will study fluctuations of $h_{[\gamma N]}$ around $N\chi_\gamma^*$.

Lemma 2.2. The function $\mathscr{R}_\gamma(\chi)$ is a strictly concave function on $(-\infty; \infty)$. It attains the global maximum at the point $\chi_\gamma^* = (1-\gamma)\,l + \gamma r$.

Proof. One has

$$\mathscr{R}'_\gamma(\chi) = -i\omega_1^*(\chi) + i\omega_2^*(\chi)$$

since the saddle points $\omega_1^*(\chi)$ and $\omega_2^*(\chi)$ are solutions of

$$\frac{\partial}{\partial\omega}\{i\omega[l-\chi] + \gamma \log \Lambda(\omega)\} = 0$$

and

$$\frac{\partial}{\partial\omega}\{i\omega[\chi - r] + (1-\gamma)\log \Lambda(\omega)\} = 0$$

respectively. Therefore, the equation $\mathscr{R}'_\gamma(\chi) = 0$ is equivalent to

$$g\left(\frac{l-\chi}{\gamma}\right) = g\left(\frac{\chi - r}{1-\gamma}\right) \tag{2.13}$$

Due to the monotonicity of $g(x)$ the only stationary point of $\mathscr{R}_\gamma(\chi)$ is given by

$$\chi_\gamma^* = (1-\gamma)\,l + \gamma r \tag{2.14}$$

Finally,

$$\mathscr{R}''_\gamma(\chi) = -\frac{1}{\gamma}\,g'\left(\frac{l-\chi}{\gamma}\right) - \frac{1}{1-\gamma}\,g'\left(\frac{\chi - r}{1-\gamma}\right)$$

and Lemma 2.1 yields $\mathscr{R}''_\gamma(\chi) < 0$. Therefore the stationary point χ_γ^* is the point of global maximum, and $\mathscr{R}_\gamma(\chi)$ is a strictly concave function on $(-\infty; \infty)$. ∎

Obviously

$$\omega_1^*(\chi_\gamma^*) = \omega_2^*(\chi_\gamma^*) = \omega_* = ig(l-r)$$

hence, for $Y=[\chi_\gamma^* N+\tau\sqrt{N}]$ and $X=[\gamma N]$ Eqs. (2.6) and (2.11) yield

$$Z_{X,L,Y}Z_{N-X,Y,R} = \frac{Z_{N,L,R}}{\sqrt{-2\pi N\gamma(1-\gamma)\,\Phi''(\omega_*)}}\left\{\exp\left[\frac{\tau^2}{2\gamma(1-\gamma)\,\Phi''(\omega_*)}\right]+O(N^{-1/2})\right\}$$

The following local limit theorem, therefore, holds true for the sequence of the random variables $h_{[\gamma N]}$ as $N\to\infty$

$$\Pr(h_{[\gamma N]}=[\chi_\gamma^* N+\tau\sqrt{N}]) = \frac{1}{\sqrt{2\pi\gamma(1-\gamma)\,vN}}\exp\left[-\frac{\tau^2}{2\gamma(1-\gamma)\,v}\right]+O(N^{-1}) \tag{2.15}$$

where $v=-\Phi''(\omega_*)$. Equation (2.15) was derived previously in ref. 9 using a somewhat different technique.

The joint distribution of the random variables h_j and h_k where $j<k$, $j=[\gamma N]$, $k=[\eta N]$ (or, indeed, of any finite set $\{h_j\}_{j\in A}$) can be calculated in much the same way. First note that

$$\Pr(h_j=x;\,h_k=y)=\frac{Z_{j,L,x}Z_{k-j,x,y}Z_{N-k,y,R}}{Z_{N,L,R}} \tag{2.16}$$

Using Eqs. (2.6) and the steepest descent method, see ref. 11, we obtain the local limit theorem

$$\Pr(h_{[\gamma N]}=[\chi_\gamma^* N+\tau\sqrt{N}];\,h_{[\eta N]}=[\chi_\eta^* N+\sigma\sqrt{N}]) = \frac{1}{2\pi Nv\sqrt{\gamma(\eta-\gamma)(1-\eta)}}\exp\left\{-\frac{1}{2v}\left[\frac{\tau^2}{\gamma}+\frac{(\tau-\sigma)^2}{\eta-\gamma}+\frac{\sigma^2}{1-\eta}\right]\right\} + O(N^{-3/2})$$

The corresponding two dimensional central limit theorem is stated as follows

$$\lim_{N\to\infty}\Pr(\zeta_{[\gamma N]}\leqslant\tau;\,\zeta_{[\eta N]}\leqslant\sigma) = \frac{1}{2\pi\sqrt{\gamma(\eta-\gamma)(1-\eta)}}\int_{-\infty}^{\tau}\int_{-\infty}^{\sigma}du\,dv\exp\left\{-\frac{1}{2}\left[\frac{u^2}{\gamma}+\frac{(u-v)^2}{\eta-\gamma}+\frac{v^2}{1-\eta}\right]\right\} \tag{2.17}$$

In particular the correlation coefficients of the random variables $\phi_\gamma \stackrel{d}{=} \lim_{N\to\infty} \zeta_{[\gamma N]}$ are given by

$$\rho(\phi_\gamma; \phi_\eta) = \sqrt{\frac{\gamma(1-\eta)}{\eta(1-\gamma)}} \tag{2.18}$$

where $\gamma < \eta$. Note that there is virtually no correlation decay in the model—macroscopically separated random variables $\zeta_{[\gamma N]}$ and $\zeta_{[\eta N]}$ have non-vanishing correlation coefficient.

2.2. Macroscopic Shape of the Interface

Equations (2.14) and (2.15) provide detailed description of the local properties of the SOS interface (2.1). Our goal now is to describe the global shape of the interface (2.1) in the macroscopic scale (that is, in the continuum limit). Using the inequality (exponential tightness, see ref. 11)

$$\Pr\{\boldsymbol{h}_{N-1}: |h_k - Y^*_{k/N}| \geqslant \varepsilon N\} \leqslant C_\varepsilon N^{-1/2} e^{-N\alpha\varepsilon^2/2}$$

one obtains

$$\Pr\left[\bigcap_{k=1}^{N-1} \{\boldsymbol{h}_{N-1}: |h_k - Y^*_{k/N}| \leqslant \varepsilon N\}\right] \geqslant 1 - \sum_{k=1}^{N-1} \Pr\{\boldsymbol{h}_{N-1}: |h_k - Y^*_{k/N}| \geqslant \varepsilon N\}$$
$$\geqslant 1 - C_\varepsilon N^{1/2} e^{-N\alpha\varepsilon^2/2} \tag{2.19}$$

where $Y^*_\gamma = L(1-\gamma) + R\gamma$. Therefore, for any $\varepsilon > 0$,

$$\Pr[\sup_{\gamma\in[0;1]} |N^{-1} h_{[N\gamma]} - h(\gamma)| < \varepsilon] \to 1$$

as $N \to \infty$, where

$$h(\gamma) = (1-\gamma)\, l + \gamma r, \quad \gamma \in [0; 1] \tag{2.20}$$

That is, for any positive ε and δ the rescaled interfaces $N^{-1} h_{[N\gamma]}$, $\gamma \in [0; 1]$ belong to the ε-vicinity of the function $h(\gamma)$ if N is large enough, except for a set of atypical interfaces which probability is less then δ. In this sense the typical interfaces $\boldsymbol{h}_{N-1}$ of the model (2.1) *merge* into the function $h(\gamma)$ in the continuum limit.

Let us also mention a result concerning the large deviation probabilities for the random configuration $\{h_k\}_{k=1}^{N-1}$. Let $\eta(x)$ be a continuous function defined on the interval $[0; 1]$, and $\eta(0) = l$, $\eta(1) = r$, then

$$\lim_{N\to\infty}\frac{1}{N}\log \Pr[\boldsymbol{h}_{N-1}: \max_{k=1,\ldots,N-1}|h_k - N\eta(k/N)| \leqslant N\varepsilon]$$

$$= -\beta \inf_{\psi(\tau)}\left\{\int_0^1 f_\beta(\psi'(\tau))\,d\tau: \sup_{\tau\in[0;1]}|\psi(\tau)-\eta(\tau)|\leqslant\varepsilon\right\} + \beta f_\beta(l-r) \quad (2.21)$$

where $f_\beta(x)$ is given by Eq. (2.9), and the infimum is taken over the set of continuously differentiable functions C^1 such that $\psi(0)=l$ and $\psi(1)=r$. The integral $\int_0^1 f_\beta(\psi'(\tau))\,d\tau$ is the total free energy associated with the interface $\psi(\tau)$.

Note that the rate function $\mathscr{R}_\gamma(\chi)$ given by Eq. (2.12) can be also expressed in terms of a constrained infimum of the total free energy. Using the arguments from the proof of Lemma 2.2 one can show that

$$\mathscr{R}_\gamma(\chi) = -\beta \inf_{\psi(\tau)}\left\{\int_0^1 f_\beta[\psi'(\tau)]\,d\tau: \psi(\gamma)=\chi\right\}$$

where as above the infimum is taken over the C^1 functions $\psi(\cdot)\colon [0;1]\to(-\infty;\infty)$ such that $\psi(0)=l$, $\psi(1)=r$. The infimum is attained at the piecewise linear function

$$\psi_\gamma(\tau) = \begin{cases} l-\tau(l-\chi)/\gamma, & \tau\in[0;\gamma] \\ \tau(r-\chi)/(1-\gamma)-(r\gamma-\chi)/(1-\gamma), & \tau\in[\gamma;1] \end{cases} \quad (2.22)$$

Using Eq. (2.10) and (2.20) one can conclude that for any $\varepsilon>0$

$$\Pr[\sup_{\tau\in[0;1]}|N^{-1}h_{[\tau N]}-\psi_\gamma(\tau)|<\varepsilon \mid h_{[\gamma N]}=[\chi N]]\to 1 \quad (2.23)$$

as $N\to 0$, where $\Pr[\cdot\,|h_{[\gamma N]}=[\chi N]]$ is the distribution (2.1) conditioned by $h_{[\gamma N]}=[\chi N]$. That is, the typical interfaces $\boldsymbol{h}_{N-1}$ realizing the large deviation $h_{[\gamma N]}=[\chi N]$ merge into the function $\psi_\gamma(\tau)$ in the continuum limit.

3. SOS INTERFACE NEAR AN ATTRACTING WALL

The state space of the height variables in this version of the SOS model is the set of non-negative integers $Z_+\equiv\{0,1,2,\ldots\}$. The joint distribution of the sequence of height variables $\boldsymbol{h}_{N-1}\equiv\{h_j\}_{j=1}^{N-1}$ is given by

$$\mathbf{P}(\boldsymbol{h}_{N-1}) = \Theta_{N,L,R}^{-1}\exp\left[-\beta J\sum_{j=1}^{N}|h_j-h_{j-1}|+\beta b\sum_{j=1}^{N-1}\delta(h_j;0)\right] \quad (3.1)$$

where $h_j \in Z_+$, $\forall j$; $J>0$, $b>0$, and $h_0=L$, $h_N=R$ (the boundary conditions).

3.1. The Integral Representation for the Partition Function

The partition function $\Theta_{N,L,R}$ is given by

$$\Theta_{N,L,R}=\sum_{h_1,\ldots,h_N=0}^{\infty}\exp\left[-\beta J\sum_{j=1}^{N}|h_j-h_{j-1}|+\beta b\sum_{j=1}^{N-1}\delta(h_j;0)\right]\delta(h_N;R) \tag{3.2}$$

It can be expressed in terms of the transfer operator $\hat{F}$ acting in l_2

$$[\hat{F}\psi]_j=e^{(1/2)\beta b\,\delta(j;0)}\sum_{l=0}^{\infty}e^{-\beta J|j-l|+(1/2)\beta b\,\delta(l;0)}\psi_l \tag{3.3}$$

Indeed, Eqs. (3.2) and (3.3) yield

$$\Theta_{N,L,R}=(\delta_L,\hat{F}^N\delta_R)\,e^{-(1/2)\beta b[\delta(L;0)+\delta(R;0)]} \tag{3.4}$$

where $(\cdot,\cdot)$ is the usual scalar product in l_2, and $\delta_L=\{\delta(j;L)\}_{j=0}^{\infty}\in l_2$.

It is convenient to introduce truncated operators $\hat{F}_k$ via

$$[\hat{F}_k\psi]_j=\begin{cases}e^{(1/2)\beta b\,\delta(j;0)}\sum_{l=0}^{k}e^{-\beta J|j-l|+(1/2)\beta b\,\delta(l;0)}\psi_l, & \text{if } j\in\{0,1,\ldots,k\}\\ 0, & \text{otherwise}\end{cases}$$

An almost verbatim repetition of the arguments used in ref. 11 shows that

$$\lim_{k\to\infty}(\delta_L,\hat{F}_k^N\delta_R)=(\delta_L,\hat{F}^N\delta_R) \tag{3.5}$$

and, once $k>\max(L,R)$,

$$(\delta_L,\hat{F}_k^N\delta_R)=\sum_{n=1}^{k+1}\Lambda_n^N v_{n,L}^{(k)}v_{n,R}^{(k)} \tag{3.6}$$

where $\{\Lambda_n\}_{n=1}^{k+1}$, and $v_n^{(k)}=\{v_{n,j}^{(k)}\}_{j=0}^{k}$, $n=1,2,\ldots,k+1$ are the eigenvalues and the associated eigenvectors of the matrices

$$\hat{W}_k\equiv\{w_{j,l}\}_{j,l=0}^{k}=\{e^{-\beta J|j-l|+\beta b[\delta(j;0)+\delta(j;0)]/2}\}_{j,l=0}^{k}$$

It can be shown by the methods used in Appendix that when $e^{-\beta J} \geqslant 1 - e^{-\beta b}$ the eigenvalues of the matrix $\hat{W}_k$ are given by

$$\Lambda_n = \frac{\sinh \beta J}{\cosh \beta J - \cos \varphi_n}, \qquad n = 1, 2, \ldots, k+1 \tag{3.7}$$

where $\varphi_n \in [0; 2\pi)$ are solutions of

$$e^{i(2k+1)\varphi} = \frac{1 - e^{i\varphi} e^{\beta J}(1 - e^{-\beta b})}{e^{i\varphi} - e^{\beta J}(1 - e^{-\beta b})} \left(\frac{1 - e^{i\varphi} e^{-\beta J}}{e^{i\varphi} - e^{-\beta J}} \right)^2 \tag{3.8}$$

The corresponding orthonormal eigenvectors are given by

$$\psi_j = \left\{ e^{\beta b\, \delta(l;0)/2} \frac{A_j \exp(il\varphi_j) - A_j^{-1} \exp(-il\varphi_j)}{i\sqrt{2(k+1)}} [1 + O(k^{-1})] \right\}_{l=0}^{k} \tag{3.9}$$

$j = 1, 2, \ldots, k+1$; where

$$A_j^2 = \nu(\varphi_j) \equiv \frac{e^{i\varphi_j} - e^{-\beta J}}{1 - e^{i\varphi_j} e^{-\beta J}} \frac{1 - e^{i\varphi_j} \xi_2}{e^{i\varphi_j} - \xi_2} \tag{3.10}$$

and $\xi_{1,2} = \exp\{\pm[\beta J + \log(1 - e^{-\beta b})]\}$.

When $e^{-\beta J} < 1 - e^{-\beta b}$ only the first k eigenvalues are given by Eq. (3.7) (With the associated eigenvectors given by Eq. (3.9)). The remaining $k+1$-st eigenvalue is given by (up to an irrelevant exponentially small with k correction)

$$\Lambda_{k+1} = \frac{\sinh \beta J}{\cosh \beta J - \cosh(\log \xi_2)}$$

The corresponding eigenvector is given by (up to an irrelevant $O(e^{-\gamma k})$ correction)

$$\psi_{k+1} = \left\{ [1 + \delta(l;0)(e^{\beta b/2} - 1)] \left(e^{\beta b} + \frac{1}{\xi_1^2 - 1} \right)^{-1/2} \xi_2^l \right\}_{l=0}^{k}$$

It turns out that the solutions of Eq. (3.8) are such that $e^{i\varphi_k}$ are virtually uniformly distributed over the unit circle (cf., Lemma A2 from Appendix). This fact together with Eqs. (3.4)–(3.7), and (3.9) yield in the

limit $k \to \infty$ the following integral representations for the partition function (3.2). When $e^{-\beta J} \geqslant 1 - e^{-\beta b}$,

$$\Theta_{N,L,R} = \frac{1}{2\pi} \int_{-\pi}^{\pi} d\omega \, \Lambda^N(\omega) [e^{i\omega(L-R)} - \nu(\omega) \, e^{i\omega(L+R)}] \equiv Z_{N,L,R} - J_{N,L,R} \tag{3.11}$$

where $\Lambda(\omega)$ is given by Eq. (2.5), $\nu(\omega)$ is given by Eq. (3.10), and $Z_{N,L,R}$ is the partition function of the SOS interface (2.1).

When $e^{-\beta J} < 1 - e^{-\beta b}$

$$\Theta_{N,L,R} = \mathscr{D}_{N,L,R} + Z_{N,L,R} - J_{N,L,R} \tag{3.12}$$

where

$$\mathscr{D}_{N,L,R} \equiv [e^{\beta b} + (\xi_1^2 - 1)^{-1}]^{-1} \, \xi_2^{L+R} \left[\frac{\sinh \beta J}{\cosh \beta J - \cosh(\log \xi_2)} \right]^N$$

is the contribution from the point spectrum of the operator $\hat{F}$.

3.2. The Asymptotic Expansion for the Partition Function

When $e^{-\beta J} > 1 - e^{-\beta b}$, the large N asymptotic expansion for the integral $J_{N,L,R}$ can be derived using the steepest descent method, see ref. 11. Indeed, in addition to the poles at $\omega = \pm i\beta J$ the integrand of $J_{N,L,R}$ has an extra pole at $\omega_0 = -i \log \xi_2$. However, when $e^{-\beta J} > 1 - e^{-\beta b}$ the extra pole is in the lower half-plane and one can still deform the original integration contour (the segment $[-\pi; \pi]$) into the steepest descent path without crossing the poles. For $L = [lN]$, $R = [rN]$ we obtain

$$J_{N,L,R} = \frac{\Lambda^N(\omega_+^*) \, e^{-(L+R) \, g(l+r)}}{\sqrt{-2\pi N \Phi''(\omega_+^*)}} [\nu(\omega_+^*) + O(N^{-1})] \tag{3.13}$$

where $\omega_+^* = ig(l+r)$, see Eq. (2.7), and $\nu(x)$ is given by Eq. (3.10).

Consider now the case $e^{-\beta J} < 1 - e^{-\beta b}$. In this case the integrand in $J_{N,L,R}$ has a pole in the upper half-plane at $\omega_0 = i[\beta J + \log(1 - e^{-\beta b})]$, and if the saddle point $\omega_+^* \equiv ig(l+r)$ is above or coincides with ω_0 the pole plays quite a non-trivial role, as we shall see below. The condition $\omega_+^* = \omega_0$ implies

$$e^{-g(l+r)} = \frac{e^{-\beta J}}{1 - e^{-\beta b}} \equiv \xi_2$$

or, taking into account Eq. (2.7),

$$l + r = e^{\beta b} - \left[1 - \frac{e^{-2\beta J}}{1 - e^{-\beta b}} \right]^{-1} \equiv \tan \theta_c \tag{3.14}$$

Remark 3.1. It will become clear below that $\tan\theta_c$ introduced in Eq. (3.14) is $\tan(\cdot)$ of the contact angle—the angle between the wall $h_j = -1$, $j = 1,\ldots, N-1$ and the inclined parts of the interface (2.1) in the macroscopic scale.

If $l + r < \tan\theta_c$ then the saddle point ω_+^* is below the pole ω_0 and the integral $J_{N,L,R}$ is evaluated as in the case $e^{-\beta J} > 1 - e^{-\beta b}$ (that is, the original integration contour can still be deformed into the steepest descent path without crossing the pole ω_0). Therefore, Eq. (3.13) is also valid for $e^{-\beta J} < 1 - e^{-\beta b}$ provided $l + r < \tan\theta_c$. For $\omega_+^* \neq \omega_0$ one has

$$\min_{y \in (-\beta J;\, \beta J)} \log \Lambda(iy) - (l+r)\, y = \min_{y \in (-\beta J;\, \beta J)} \log \Lambda(iy) + (l+r)\, y$$

$$< \log \Lambda(i \log \xi_2) + (l+r) \log \xi_2$$

Hence if $l = 0$ or $r = 0$

$$\Theta_{N,L,R} = [e^{\beta b} + (\xi_1^2 - 1)^{-1}]^{-1}\, \xi_2^{L+R}\, \Lambda^N(i \log \xi_2)[1 + O(e^{-\varepsilon N})] \tag{3.15}$$

where $\varepsilon \equiv \varepsilon(l, r) > 0$ when $l + r < \tan\theta_c$. While if $\min(l, r) > 0$ the asymptotic expansion for $\Theta_{N,L,R}$ is given by

$$\Theta_{N,L,R} = \frac{\Lambda^N(i \log \xi_2)}{e^{\beta b} + (\xi_1^2 - 1)^{-1}}\, \xi_2^{L+R}$$

$$+ \frac{\Lambda^N(\omega_-^*)}{\sqrt{-2\pi N \Phi''(\omega_-^*)}}\, e^{i(L-R)\omega^*}[1 + O(N^{-1})] \tag{3.16}$$

Depending on the exact values of the parameters l, r, βJ, βb, either the first or the second term in the rhs of Eq. (3.16) gives the leading term in the asymptotic expansion for $\Theta_{N,L,R}$. We call Phase I the range of parameters where $\mathscr{D}_{N,L,R}$ dominates over the contribution from the continuous spectrum. The complementary region is called Phase II. The dominance interchange which occurs at the hypersurface (phase boundary)

$$\min_{y \in (-\beta J;\, \beta J)} [\log \Lambda(iy) - (l-r)\, y] = (l+r) \log \xi_2 + \log \Lambda(i \log \xi_2) \tag{3.17}$$

gives rise to a nonanalyticity of the infinite volume free energy per site

$$f(\beta) = -\lim_{N \to \infty} \frac{1}{\beta N} \log \Theta_{N,L,R}$$

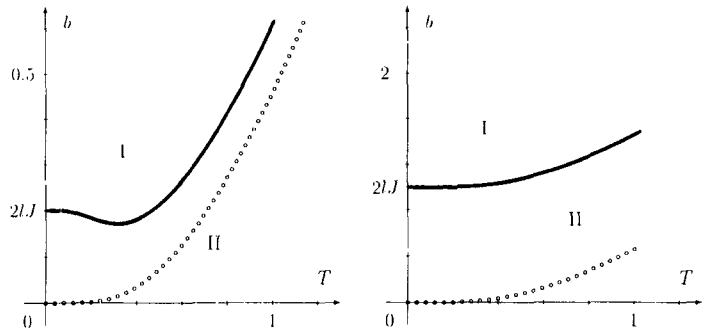

Fig. 1. The $b-T$ phase diagram for the SOS interface near an attracting wall. The values of parameters are $l=r=0.1$, $J=1$ (left) and $l=r=0.5$, $J=1$ (right). In Phase I the interface has contact with the wall at a macroscopically large number of points. In Phase II the interface is the straight line joining the boundary points $L=[lN]$ and $R=[rN]$. The circles show the coexistence line in the case $l=r=0$.

For instance, in the case $l=r$ the critical height l_{cr} is given by

$$l_{cr}=\frac{1}{2\log\xi_2}\log\frac{\cosh\beta J-\cosh(\log\xi_2)}{\cosh\beta J-1} \tag{3.18}$$

and

$$-\beta f(\beta)=\begin{cases}2l\log\xi_2+\log A(i\log\xi_2), & \text{if } l<l_{cr}\\ \log\coth(\beta J/2), & \text{if } l>l_{cr}\end{cases}$$

See Figs. 1 and 2 for $b-T$ phase diagrams.

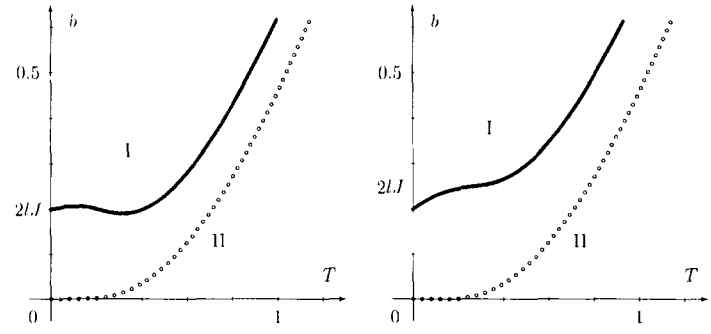

Fig. 2. The $b-T$ phase diagram for the SOS interface near an attracting wall. The values of parameters are $l=0.1$, $r=0.12$, $J=1$ (left) and $l=0.1$, $r=0.2$, $J=1$ (right). The Phases I and II are the same as in Fig. 1. The circles show the coexistence line in the case $l=r=0$. Note that in the case $l=0.1$, $r=0.12$ the line $b=\text{const}$ can cross the coexistence line at three points.

For the purpose of later use we introduce the notation $r_{cr}(l)$ to denote (for $l \leqslant \tan \theta_c$) the critical value of r—the unique solution of the Eq. (3.17) with respect to the variable r.

Remark 3.2. The existence of the limit $N \to \infty$ for the free energies $f_N(\beta)$ implies that taking the limit $N \to \infty$ in the systems of the size $[\gamma N]$ with the boundary conditions $L = [\gamma l N]$, $R = [\gamma r N]$ yields the same phase diagram for all $\gamma > 0$, and, in particular, the same critical value $r_{cr}(l)$ for the parameter r. Therefore, taking the limit $N \to \infty$ in the systems of the size $[\gamma N]$ with the boundary conditions $L = [lN]$, $R = [rN]$ yields a phase diagram with the critical value of r given by $\gamma r_{cr}(l/\gamma)$ if $l \leqslant \gamma \tan \theta_c$ (otherwise r does not have a critical value).

Let, now, $l + r > \tan \theta_c$, that is the pole ω_0 is in the upper half-plane and is below the saddle point ω_+^*. The integral $J_{N,L,R}$ can be represented as

$$J_{N,L,R} = \frac{1}{2\pi} \int_{C_N} d\omega \, \Lambda^N(\omega) \, e^{i\omega(L+R)} \nu(\omega) + [e^{\beta b} + (\xi_1^2 - 1)^{-1}]^{-1} \, \xi_2^{L+R} \Lambda^N(i \log \xi_2) \tag{3.19}$$

where the second term is the residue of the integrand at $\omega = \omega_0$ times $2\pi i$, and C_N is the steepest descent path. Note that $\mathscr{Q}_{N,L,R}$ (the point spectrum contribution to the partition function) and the pole contribution in Eq. (3.19) cancel each other in Eq. (3.12). The integral in Eq. (3.19) is evaluated by the steepest descent method, which yields the expression given by the rhs of Eq. (3.13). The asymptotic expansion for $\Theta_{N,L,R}$ is now readily obtained from Eqs. (3.12), (3.19), and (2.6). In the case $l, r > 0$ it reduces to

$$\Theta_{N,L,R} = \frac{1}{\sqrt{-2\pi N \Phi''(\omega_-^*)}} \exp\left\{ N \min_{y \in (-\beta J; \beta J)} [\log \Lambda(iy) - (l - r) y] \right\} \times [1 + O(N^{-1})] \tag{3.20}$$

3.3. Macroscopic Shape of the Interface: Unpinned State

We have

$$\Pr[h_X = Y] = \frac{\Theta_{X,L,Y} \Theta_{N-X,Y,R}}{\Theta_{N,L,R}} \, e^{\beta b \, \delta(Y;0)} \tag{3.21}$$

It is easy to see from Eqs. (3.11) and (3.13), and the results of Sections 2, that if $e^{-\beta J} > 1 - e^{-\beta b}$ the large N properties of the interface (3.1) are essentially the same as in the case considered in Section 2 (that is, when $e^{-\beta J} > 1 - e^{-\beta b}$ the temperature fluctuations overwhelm the attraction of the wall). Therefore below we consider only the case $e^{-\beta J} \leqslant 1 - e^{-\beta b}$.

We consider first the boundary conditions $L = [lN]$, R is finite and fixed, and choose $l > \tan\theta_c$, see Eq. (3.14). As $N \to \infty$ the distribution of a random variable $h_{[\gamma N]}/N$, where $\gamma \in [0; 1]$, concentrates at a certain value $\chi = \chi_\gamma^*$ which, as Eq. (3.21) suggests, is the maximum point of the rate function $\mathscr{R}_\gamma(\chi)$ of $\Theta_{[\gamma N], L, [\chi N]} \Theta_{N-[\gamma N], [\chi N], R}$ on $[0; \infty)$. Since $(l+\chi)/\gamma \geqslant l > \tan\theta_c$ for $\chi \geqslant 0$, the leading asymptotic term of the partition function $\Theta_{[\gamma N], L, [\chi N]}$ is given by an expression analogous to Eq. (3.20), namely,

$$\Theta_{[\gamma N], L, [\chi N]} = \frac{\Lambda^{[\gamma N]}(\omega_-^*)}{\sqrt{-2\pi\gamma N \Phi''(\omega_-^*)}} e^{i\omega^* (L - [\chi N])} [1 + O(N^{-1})] \quad (3.22)$$

where $\omega_-^* = ig[(l-\chi)/\gamma]$, see Eq. (2.7). Depending on the exact value of χ the partition function $\Theta_{N-[\gamma N], [\chi N], R}$ is given by an expression analogous to either Eq. (3.15) or Eq. (3.20). Namely, if $\chi > \chi_s \equiv (1-\gamma)\tan\theta_c$ then

$$\Theta_{N-[\gamma N], [\chi N], R} = \frac{\Lambda^{N-[\gamma N]}(\omega_-^{**})\, e^{i\omega_-^{**}[\chi N]}}{\sqrt{-2\pi(1-\gamma)\, N\Phi''(\omega_-^{**})}} [e^{-i\omega_-^{**}R} - \nu(\omega_-^{**})\, e^{i\omega_-^{**}R} + O(N^{-1})] \quad (3.23)$$

where $\omega_-^{**} = ig[\chi/(1-\gamma)]$, and

$$\Theta_{N-[\gamma N], [\chi N], R} = [e^{\beta b} + (\xi_1^2 - 1)^{-1}]^{-1}\, \xi_2^{[\chi N]+R} \Lambda^{N-[\gamma N]}(i\log\xi_2)[1 + O(e^{-\varepsilon N})] \quad (3.24)$$

if $\chi < \chi_s$. Therefore, the rate function $\mathscr{R}_\gamma(\chi)$ is given by

$$\mathscr{R}_\gamma(\chi) = \begin{cases} R_1(\chi), & \text{for } \chi \in [0; (1-\gamma)\tan\theta_c] \\ R_2(\chi), & \text{for } \chi \in [(1-\gamma)\tan\theta_c; \infty) \end{cases} \quad (3.25)$$

see Fig. 3, where

$$R_1(\chi) = \min_{y \in (-\beta J; \beta J)} [\gamma \log \Lambda(iy) - (l-\chi)\, y] + (1-\gamma)\log\Lambda(i\log\xi_2) + \chi\log\xi_2 \quad (3.26)$$

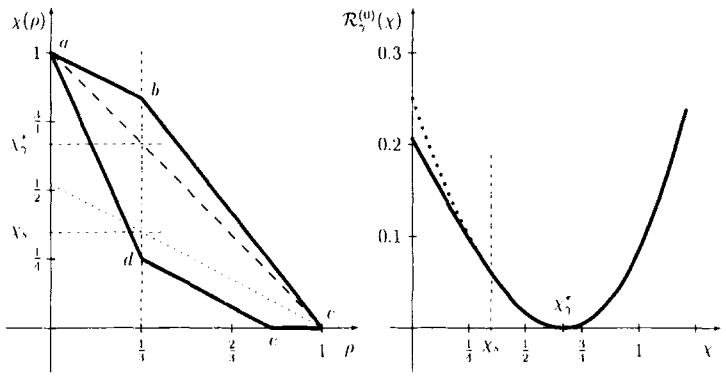

Fig. 3. The typical interfaces realizing large deviations $h_{\lfloor \gamma N \rfloor} = [\chi N]$ for the SOS interface (4.1) (left) and the corresponding rate function $\mathscr{R}_\gamma^{(0)}(\chi) \equiv -\mathscr{R}_\gamma(\chi) - \beta f_\beta(l)$ (right). The values of parameters are $\beta J = 1$, $\beta b = 0.65$, $\gamma = \frac{1}{3}$, $l = 1$, $r = 0$. The interfaces *abc* and *adec* correspond to $\chi = \frac{5}{6}$ and $\chi = \frac{1}{4}$, respectively. The interface *ac* is the equilibrium shape interface. The dotted line marks the critical deformation χ_s below which a part of the typical inteface- the segment *ec*—is pinned to the attracting wall. The broken line on the right figure marks the point of nonanalyticity of $\mathscr{R}_\gamma^{(0)}(\chi)$. The dots on the left from that line show the analytical continuation of $\mathscr{R}_\gamma^{(0)}(\chi)$—the rate function of the free SOS interface (2.1).

and

$$R_2(\chi) = \min_{y \in (-\beta J;\, \beta J)} [\gamma \log \Lambda(iy) - (l - \chi) y]$$

$$+ \min_{y \in (-\beta J;\, \beta J)} [(1 - \gamma) \log \Lambda(iy) - \chi y] \tag{3.27}$$

The proof of Lemma 3.1 can be found in ref. 11.

Lemma 3.1. Let $l > \tan \theta_c$, then the function $\mathscr{R}_\gamma(\chi)$ is a strictly concave and continuously differentiable function on $[0; \infty)$. It attains the global maximum at the point $\chi_\gamma^* = (1 - \gamma) l$.

To find the macroscopic shape of the interface we use the inequality (exponential tightness, see ref. 11)

$$\Pr[\boldsymbol{h}_{N-1} : |h_k - (1 - k/N) L| \geqslant \varepsilon N] \leqslant c_\varepsilon N^{-1/2} \exp(-\tfrac{1}{2} \alpha \varepsilon^2 N)$$

where $\alpha > 0$, and $0 < c_\varepsilon < \infty$ for $\varepsilon > 0$. Moreover α and c_ε do not depend on k. Therefore, cf. Eq. (2.19),

$$\Pr\left[\bigcap_{k=1}^{N} \{\boldsymbol{h}_{N-1} : |h_k - (1 - k/N) L| \leqslant \varepsilon N\} \right] \geqslant 1 - c_\varepsilon \sqrt{N}\, e^{-N \alpha \varepsilon^2 / 2}$$

That is, in the continuum limit the typical interfaces of the model (3.1) merge into the function

$$h(\gamma) = l(1-\gamma), \quad \gamma \in [0; 1] \tag{3.28}$$

since according to the above inequality for any $\varepsilon > 0$

$$\Pr[\sup_{\gamma \in [0; 1]} |h(\gamma) - N^{-1} h_{[\gamma N]}| < \varepsilon] \to 1 \tag{3.29}$$

as $N \to \infty$. Thus, if one end of the interface is raised sufficiently high ($l > \tan \theta_c$) the (typical) large N behavior of the interface (3.1) is virtually indistinguishable from the case of the "free" interface (2.1).

3.4. Macroscopic Shape of the Interface: Pinned State

Consider now the case $l < \tan \theta_c$. As above, we first have to find the value of χ maximizing $\mathscr{R}_\gamma(\chi)$—the rate function of the product $\Theta_{[\gamma N], L, [\chi N]}$ $\Theta_{N-[\gamma N], [\chi N], R}$. Now the leading asymptotic term of $\Theta_{[\gamma N], L, [\chi N]}$ is given by (cf. Eqs. (3.16) and (3.20))

$$\Theta_{[\gamma N], L, [\chi N]} = \mathscr{D}_{[\gamma N], L, [\chi N]}[1 + O(e^{-\varepsilon N})] \tag{3.30}$$

if $l < \gamma \tan \theta_c$, and $\chi < \gamma r_{cr}(l/\gamma)$, see Remark 4.2, otherwise

$$\Theta_{[\gamma N], L, [\chi N]} = \frac{\Lambda^{[\gamma N]}(\omega_-^*)\, e^{i\omega_-^*(L-[\chi N])}}{\sqrt{-2\pi\gamma N \Phi''(\omega_-^*)}}[1 + O(N^{-1})] \tag{3.31}$$

The partition function $\Theta_{N-[\gamma N], [\chi N], R}$ is still given by Eq. (3.24). Therefore the rate function $\mathscr{R}_\gamma(\chi)$ is given by

$$\mathscr{R}_\gamma(\chi) = \begin{cases} R_1(\chi), & \text{if } \chi \in [0; (1-\gamma)\tan\theta_c] \\ R_2(\chi), & \text{if } \chi \in [(1-\gamma)\tan\theta_c; \infty) \end{cases} \tag{3.32}$$

when $0 \leqslant \gamma \leqslant l/\tan\theta_c$;

$$\mathscr{R}_\gamma(\chi) = \begin{cases} R_3(\chi), & \text{if } \chi \in [0; \gamma r_{cr}(l/\gamma)] \\ R_1(\chi), & \text{if } \chi \in [\gamma r_{cr}(l/\gamma); (1-\gamma)\tan\theta_c] \\ R_2(\chi), & \text{if } \chi \in [(1-\gamma)\tan\theta_c; \infty) \end{cases} \tag{3.33}$$

when $l/\tan\theta_c \leqslant \gamma \leqslant \gamma_0$; and

$$\mathscr{R}_\gamma(\chi) = \begin{cases} R_3(\chi), & \text{if } \chi \in [0; (1-\gamma)\tan\theta_c] \\ R_4(\chi), & \text{if } \chi \in [(1-\gamma)\tan\theta_c; \gamma r_{cr}(l/\gamma)) \\ R_2(\chi), & \text{if } \chi \in [\gamma r_{cr}(l/\gamma); \infty) \end{cases} \tag{3.34}$$

when $\gamma_0 \leqslant \gamma \leqslant 1$. In the above expressions γ_0 is the unique solution of $\gamma r_{cr}(l/\gamma) = (1-\gamma)\tan\theta_c$ (note that $\gamma_0 \in [(1+l/\tan\theta_c)/2; 1]$), the functions $R_1(\chi)$ and $R_2(\chi)$ are given by Eqs. (3.26) and (3.27), respectively, and

$$R_3(\chi) = \log \Lambda(i \log \xi_2) + (l + 2\chi)\log \xi_2$$

$$R_4(\chi) = \gamma \log \Lambda(i \log \xi_2) + (l+\chi)\log \xi_2 + \min_{y \in (-\beta J; \beta J)} [(1-\gamma)\log \Lambda(iy) - \chi y]$$

The proof of Lemma 3.2 can be found in ref. 11.

Lemma 3.2. Let $l < \tan\theta_c$, then the rate function $\mathscr{R}_\gamma(\chi)$ given by Eqs. (3.32), (3.33), and (3.34) has the following properties. When $0 < \gamma \leqslant l/\tan\theta_c$, $\mathscr{R}_\gamma(\chi)$ is strictly concave, continuously differentiable and attains the global maximum at $\chi = l - \gamma\tan\theta_c$. When $l/\tan\theta_c \leqslant \gamma < 1$, $\mathscr{R}_\gamma(\chi)$ is a decreasing and continuous function on $[0; \infty)$.

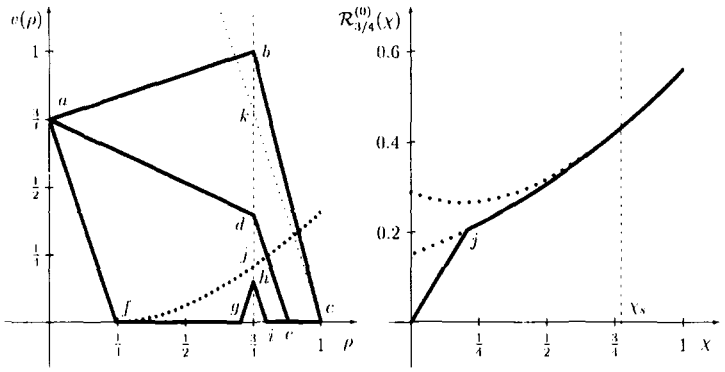

Fig. 4. The typical interfaces realizing large deviations $h_{\lfloor \gamma N \rfloor} = \lfloor \chi N \rfloor$ for the SOS interface (4.1) (left) and the corresponding rate function $\mathscr{R}^{(0)}_\gamma(\chi) \equiv -\mathscr{R}_\gamma(\chi) + \beta f_\beta(l)$ (right). The values of parameters are $\beta J = 3/4$, $\beta b = 3/2$, $\gamma = 3/4$, $l = 3/4$, $r = 0$. The small dots mark the critical deformation $\chi_s = (1-\gamma)\tan\theta_c$ below which the right wing of the typical interface is pinned to the attracting wall—the segment ec. The big dots (on the left picture) mark the critical deformation below which the left wing of the typical interface—the segment fg—is pinned to the attracting wall.

Summarizing the above, one concludes that in the case $l < \tan\theta_c$ the maximum point of the rate function $\mathscr{R}_\gamma(\chi)$ on the interval $[0; \infty)$ is given by

$$\chi_\gamma^* = \begin{cases} l - \gamma \tan\theta_c, & \text{for } 0 \leqslant \gamma \leqslant l/\tan\theta_c \\ 0, & \text{for } l/\tan\theta_c \leqslant \gamma \leqslant 1 \end{cases} \tag{3.35}$$

Although in the case $l < \tan\theta_c$ the rate function $\mathscr{R}_\gamma(\chi)$ is not necessarily concave it always consists from two concave pieces and has a unique maximum, see Fig. 4. We have (exponential tightness, see ref. 11)

$$\Pr[\mathbf{h}_{N-1}: |h_k - N\chi_{k/N}^*| \geqslant \varepsilon N] \leqslant c_\varepsilon N^{-1/2} \exp(-\tfrac{1}{2}\alpha\varepsilon^2 N)$$

where $\alpha > 0$, $0 < c_\varepsilon < \infty$ (for $\varepsilon > 0$) do not depend on k. Using elementary inequalities, the same as in Eq. (2.19), we conclude that

$$\Pr\left[\bigcap_{k=1}^{N-1} \{\boldsymbol{h}_{N-1}: |h_k - N\chi_{k/N}^*| \leqslant \varepsilon N\}\right] \geqslant 1 - c_\varepsilon \sqrt{N}\, e^{-N\alpha\varepsilon^2/2}$$

That is, when $e^{-\beta J} < 1 - e^{-\beta b}$, $l < \tan\theta_c$, and $r = 0$ the typical interfaces of the model (3.1) merge in the continuum limit into the function

$$h(\rho) = \begin{cases} l - \rho \tan\theta_c, & \text{for } 0 \leqslant \rho \leqslant l/\tan\theta_c \\ 0, & \text{for } l/\tan\theta_c \leqslant \rho \leqslant 1 \end{cases} \tag{3.36}$$

in the sense of Eq. (3.29).

3.5. Large Deviations of Pinned Interface

The rate functions (2.12), (3.25), and (3.32)–(3.34) show that the large N asymptotic expansions for the probabilities of rare events are significantly different in the cases $e^{-\beta J} < 1 - e^{-\beta b}$ and $b = 0$. The most noticeable difference between (2.12) and the rate functions found in the present section is the non-analyticity of the latter, see Figs. 3 and 4. The origin of the non-analyticity is the competition between different classes of the configurations $\boldsymbol{h}_N$. Consider first the case $l > \tan\theta_c$ when the rate function is given by Eq. (3.25).

The proof of the following lemma can be found in ref. 11.

Lemma 3.3. Let $l > \tan\theta_c$ and $\chi > \chi_s$, then the typical interfaces realizing the large deviation $h_{[\gamma N]} = [\chi N]$ merge in the continuum limit into the function

$$v_\chi(\rho) = \begin{cases} l - \rho(l - \chi)/\gamma, & \rho \in [0; \gamma] \\ \chi(1 - \rho)/(1 - \gamma), & \rho \in [\gamma; 1] \end{cases} \tag{3.37}$$

in the sense of Eq. (2.23). Let $l > \tan\theta_c$ and $\chi < \chi_s$, then the typical interfaces realizing the large deviation $h_{[\gamma N]} = [\chi N]$ merge into the function

$$w_\chi(\rho) = \begin{cases} l - \rho(l-\chi)/\gamma, & \rho \in [0; \gamma] \\ \chi - \tan\theta_c(\rho - \gamma), & \rho \in [\gamma; \gamma + \chi/\tan\theta_c] \\ 0, & \rho \in [\gamma + \chi/\tan\theta_c; 1] \end{cases} \tag{3.38}$$

According to Eqs. (2.22) and (3.37) the typical configurations of the interfaces (2.1) and (3.1) (with $L = [lN]$ and R is finite and fixed) realizing the large deviation $h_{[\gamma N]} = [\chi N]$ merge into the same function $v_\chi(\rho)$ in the case $\chi > \chi_s$. Since such configurations are bound to ignore the attracting wall, the rate functions (2.12) and (3.25) (which are determined by the total "weight" of the typical configurations realizing $h_{[\gamma N]} = [\chi N]$) coincide for $\chi > \chi_s$. The analytical continuation of $\mathscr{R}_\gamma$ from $\chi > \chi_s$ onto $\chi < \chi_s$ (that is, the rate function (2.12)) is determined by the total "weight" of the configurations which for $\chi < \chi_s$ still merge into the function $v_\chi(\rho)$ in the continuum limit. However the typical configurations of the model (3.1) realizing $h_{[\gamma N]} = [\chi N]$ in the case $\chi < \chi_s$ merge into the function $w_\chi(\rho)$ given by Eq. (3.38). That is, the typical configurations realizing the event $h_{[\gamma N]} = [\chi N]$ for $\chi < \chi_s$ are partially pinned to the attracting wall. These typical configurations must have a larger total "weight" then the configurations merging into $v_\chi(\rho)$, and, therefore, the rate function $\mathscr{R}_\gamma(\chi)$ given by Eq. (3.25) is larger then the rate function (2.12) for $\chi < \chi_s$. This naturally give rise to a non-analyticity of $\mathscr{R}_\gamma(\chi)$. Although, as we mentioned above, the analytic continuation of $\mathscr{R}_\gamma(\chi)$ from $\chi > \chi_s$ onto $\chi < \chi_s$ can be interpreted as a total "weight" of a certain class of interfaces, the analytic continuation of $\mathscr{R}_\gamma(\chi)$ from $\chi < \chi_s$ into $\chi > \chi_s$ does not correspond to *any* class of interfaces.

Remark 3.3. Note that the typical interfaces of the model (31) realizing $h_{[\gamma N]} = [\chi N]$ always merge into a unique function (even for $\chi = \chi_s$). The transition from the partially pinned interface $w_\chi(\rho)$ to the unpined interface $v_\chi(\rho)$ is "continuous," that is, $w_{\chi_s - \varepsilon}(\rho) \to v_{\chi_s + \varepsilon}(\rho)$ as $\varepsilon \downarrow 0$ uniformly over $\rho \in [0; 1]$. The rate function $\mathscr{R}_\gamma(\chi)$, although non-analytic at χ_s, is continuously differentiable at $\chi = \chi_s$.

3.6. The Distribution of Height Variables

In the case $l > \tan\theta_c$ the fluctuations of the interface (3.1) are the same as the fluctuations of the interface (2.1). Indeed, it follows from Lemma 3.1 and (3.25) that the fluctuations of $h_{[\gamma N]}$ around $N\chi_\gamma^*$ are controlled by the rate function $R_2(\chi)$, the same rate function as (2.12). Therefore $\Pr(h_{[\gamma N]} = [\chi_\gamma^* N + \tau\sqrt{N}])$ is given by Eq. (2.15).

Consider now the case $e^{-\beta J} \leqslant 1 - e^{-\beta b}$, $l \leqslant \tan \theta_c$ and $r = 0$. For $\gamma \in [0; l/\tan \theta_c)$ fluctuations of $h_{[\gamma N]}$ around the concentrating value $N\chi_\gamma^*$ are controlled by the rate function $R_1(\chi)$. The asymptotic expansion for $\Theta_{[\gamma N], L, [\chi_\gamma^* N + \tau\sqrt{N}]}$ is given by

$$\Theta_{[\gamma N], L, [\chi_\gamma^* N + \tau\sqrt{N}]} = \frac{\Lambda^{[\gamma N]}(i \log \xi_2)}{\sqrt{2\pi\gamma N v}} \xi_2^{L - [\chi_\gamma^* N + \tau\sqrt{N}]} \left[\exp\left(-\frac{\tau^2}{2\gamma v} \right) + O(N^{-1/2}) \right]$$

where $v = -\Phi''(i \log \xi_2)$, and

$$\Theta_{N - [\gamma N], [\chi_\gamma^* N + \tau\sqrt{N}], R} = \frac{[\Lambda(i \log \xi_2)]^{N - [\gamma N]}}{e^{\beta b} + (\xi_1^2 - 1)^{-1}} \xi_2^{R + [\chi_\gamma^* N + \tau\sqrt{N}]} [1 + O(e^{-\varepsilon N})]$$

Therefore, using Eqs. (3.21) and (3.15) one obtains

$$\Pr[h_{[\gamma N]} = [\chi_\gamma^* N + \tau\sqrt{N}]] = \frac{1}{\sqrt{2\pi\gamma v N}} \exp\left(-\frac{\tau^2}{2\gamma v} \right) + O(N^{-1}) \tag{3.39}$$

For $\gamma \in (l/\tan \theta_c; 1]$ the fluctuations are controlled by the rate function $R_3(\chi)$. The leading-order terms of $\Theta_{[\gamma N], L, k}$ and $\Theta_{N - [\gamma N], k, R}$, where k is finite and fixed, are given by

$$\Theta_{[\gamma N], L, k} \sim \frac{1}{e^{\beta b} + (\xi_1^2 - 1)^{-1}} [\Lambda(i \log \xi_2)]^{[\gamma N]} \xi_2^{L + k}$$

and

$$\Theta_{N - [\gamma N], k, R} \sim \frac{1}{e^{\beta b} + (\xi_1^2 - 1)^{-1}} [\Lambda(i \log \xi_2)]^{N - [\gamma N]} \xi_2^{k + R}$$

Therefore, see Eq. (3.21), when $\gamma \in (l/\tan \theta_c; 1]$ and $k \geqslant 0$

$$\lim_{N \to \infty} \Pr[h_{[\gamma N]} = k] = \frac{\xi_2^{2k}}{e^{\beta b} + (\xi_1^2 - 1)^{-1}} e^{\beta b\, \delta(k; 0)} \tag{3.40}$$

Note a drastic—discontinuous on the macroscopic scale—reduction in the fluctuations of

$$N^{-1/2}(h_{[\gamma N]} - N\chi_\gamma^*)$$

at $\gamma = l/\tan\theta_c$. Our goal now is to find the scale in which the reduction happens in a continuous manner, and to describe the transition in detail. The main difficulty is the calculation of the integral $J_{[\gamma N+\eta\sqrt{N}],\,L,\,\chi}$, see Eq. (3.11), where $\gamma = l/\tan\theta_c$, $L = [lN]$, and $\chi = [\rho\sqrt{N}]$. Indeed, the integrand of $J_{[\gamma N+\eta\sqrt{N}],\,L,\,\chi}$ has a saddle point at

$$\omega_N^* = -i\log\xi_2 - iN^{-1/2}\delta_* + O(N^{-1})$$

where

$$\delta_* = \frac{\tan\theta_c(\rho - \eta\tan\theta_c)}{l\Phi''(i\log\xi_2)}$$

which is sufficiently close to the pole $\omega_0 = -i\log\xi_2$ to make the standard steepest descent theorem

$$\int f(z)\,e^{NF(z)}\,dz = \sqrt{\frac{2\pi}{N\,|F''(z_*)|}}\,f(z_*)\,e^{NF(z_*)}[1 + O(N^{-1})] \tag{3.41}$$

inapplicable. However, all we need to do to obtain the correct asymptotic expansion is to apply the steepest descent method to the integral $J_{[\gamma N+\eta\sqrt{N}],\,L,\,\chi}$ (that is, to apply directly the *argument* which yield Eq. (3.41) for sufficiently regular functions $f(z)$).

We use the saddle point method in the following (not immaculate, but concise) form. Deform the original integration contour into the one passing via the saddle point and orthogonal to the imaginary axis at the saddle point (applying the residue theorem if ω_N^* is above the pole ω_0). Introduce a new integration variable y via $\omega = \omega_N^* + N^{-1/2}y$, and make standard estimates, then for $\gamma = l/\tan\theta_c$, $L = [lN]$, and $\chi = [\rho\sqrt{N}]$ one obtains

$$\begin{aligned} &J_{[\gamma N+\eta\sqrt{N}],\,L,\,\chi} \\ &\quad = [\Lambda(i\log\xi_2)]^{[\gamma N+\eta\sqrt{N}]}\,\xi_2^{L+\chi} \\ &\qquad \times\left\{\exp\left[-\frac{(\rho-\eta\tan\theta_c)^2}{2\gamma v}\right]\frac{(\xi_2 - e^{-\beta J})(\xi_1 - \xi_2)}{1-\xi_2 e^{-\beta J}}\,X(\delta_*) + O(N^{-1/2})\right\} \end{aligned}$$

where $v = -\Phi''(i\log\xi_2)$,

$$X(\delta_*) = \frac{1}{2\pi}\int_{-\infty}^{\infty}\frac{dy}{\delta_* + iy}\,e^{-\gamma v y^2/2}$$

if $\delta_* > 0$, and

$$X(\delta_*) = e^{\gamma v \delta_*^2} + \frac{1}{2\pi} \int_{-\infty}^{\infty} \frac{dy}{\delta_* + iy} e^{-\gamma v y^2/2}$$

if $\delta_* < 0$. The value of $X(0)$ can be obtained by passing to the limit $\delta_* \to 0$. The remaining integral can be expressed in terms of the error function. Indeed,

$$\frac{1}{2\pi} \int_{-\infty}^{\infty} \frac{dy}{\delta_* + iy} e^{-\alpha y^2/2} = \frac{\delta_*}{2\pi} \int_{-\infty}^{\infty} \frac{dy}{\delta_*^2 + y^2} e^{-\alpha y^2/2}$$

$$= e^{-\alpha \delta_*^2/2} \frac{\delta_*}{\sqrt{2\pi}} \int_{\sqrt{\alpha}}^{\infty} e^{-(1/2)\delta_*^2 u^2} \, du$$

where we used the identity

$$x^{-1} = \int_0^{\infty} d\tau \, e^{-\tau x}$$

to get rid of the denominator $(\delta_*^2 + y^2)^{-1}$. Therefore

$$J_{[\gamma N + \eta \sqrt{N}], L, \chi}$$

$$= [\Lambda(i \log \xi_2)]^{[\gamma N + \eta \sqrt{N}]} \xi_2^{L+\chi} \left\{ \frac{1 - \operatorname{erf}(\delta_* \sqrt{\gamma v/2})}{2[e^{\beta b} + (\xi_1^2 - 1)^{-1}]} + O(N^{-1/2}) \right\} \tag{3.42}$$

The conventional steepest descent method yields, see ref. 11,

$$Z_{[\gamma N + \eta \sqrt{N}], L, \chi}$$

$$= \frac{[\Lambda(i \log \xi_2)]^{[\gamma N + \eta \sqrt{N}]} \xi_2^{L-\chi}}{\sqrt{2\pi \gamma v N}} \left\{ \exp\left[-\frac{(\rho + \eta \tan \theta_c)^2}{2\gamma v} \right] + O(N^{-1/2}) \right\}$$

where $\gamma = l/\tan \theta_c$, $L = [lN]$, $\chi = [\rho \sqrt{N}]$, and $v = -\Phi''(i \log \xi_2)$. Note that for $\rho > 0$ only $Z_{[\gamma N + \eta \sqrt{N}], L, [\rho \sqrt{N}]}$ makes a contribution to the leading-order term of $\Theta_{[\gamma N + \eta \sqrt{N}], L, [\rho \sqrt{N}]}$.

The partition function $\Theta_{N - [\gamma N + \eta \sqrt{N}], \chi, R}$ is given by

$$\Theta_{N - [\gamma N + \eta \sqrt{N}], \chi, R} = \frac{1}{e^{\beta b} + (\xi_1^2 - 1)^{-1}} [\Lambda(i \log \xi_2)]^{N - [\gamma N + \eta \sqrt{N}]} \xi_2^{\chi + R} \tag{3.43}$$

up to an irrelevant exponentially small with N correction. Therefore for $\gamma > l/\tan\theta_c$ and $\rho > 0$ one obtains

$$\Pr[h_{[\gamma N+\sqrt{N}\eta]} = [\rho\sqrt{N}]] = \frac{1}{\sqrt{2\pi\gamma v N}} \exp\left[-\frac{(\rho+\eta\tan\theta_c)^2}{2\gamma v}\right] + O(N^{-1}) \tag{3.44}$$

If χ is kept fixed as $N \to \infty$ only $J_{[\gamma N+\eta\sqrt{N}],L,\chi}$ makes a contribution to the leading asymptotic term of $\Theta_{[\gamma N+\eta\sqrt{N}],L,\chi}$ and taking into account Eq. (3.43) one obtains

$$\lim_{N\to\infty} \Pr[h_{[Nl/\tan\theta_c+\sqrt{N}\eta]} = \chi] = \frac{\xi_2^{2\chi} e^{\beta b\,\delta(\chi;0)}}{e^{\beta b} + (\xi_1^2 - 1)^{-1}} \frac{1 + \operatorname{erf}(\eta\tan\theta_c/\sqrt{2\gamma v})}{2} \tag{3.45}$$

where χ is a non-negative integer. Note that $\lim_{N\to\infty} h_{[Nl/\tan\theta_c+\sqrt{N}\eta]}$ is an improper positive random variable.

Summarizing Eqs. (3.44) and (3.45) one concludes that the positive random variable $\lim_{N\to\infty} N^{-1/2} h_{[Nl/\tan\theta_c+\sqrt{N}\eta]}$ has an atom at the origin and

$$\lim_{N\to\infty} \Pr\left[\frac{h_{[Nl/\tan\theta_c+\sqrt{N}\eta]}}{\sqrt{N}} \leqslant \rho\right] = \frac{1}{2}\left\{1 + \operatorname{erf}\left[\frac{\rho+\eta\tan\theta_c}{\sqrt{-2l\Phi''(i\log\xi_2)/\tan\theta_c}}\right]\right\} \tag{3.46}$$

for $\rho > 0$. The "thin structure" of the atom is given by the distribution of the improper positive random variable

$$\lim_{N\to\infty} h_{[lN/\tan\theta_c+\sqrt{N}\eta]}$$

see Eq. (3.45).

Equations (3.45) and (3.46) provide comprehensive description of the interface fluctuations in the direction orthogonal to the wall. Investigation of fluctuations in the direction parallel to the wall is a significantly more delicate problem. Here we only present some intuitive arguments which allow one to derive the distribution of fluctuation of the first-contact point.

Denote j_c the point of first contact of the interface and the wall, that is, $j_c = \min\{j: h_j = 0\}$. For $j > j_c$ the interface is localized around the wall and has bounded fluctuations according to the one-sided exponential distribution (3.40), exactly as the interface (3.1) with boundary conditions $L = R = 0$. Therefore $h_j/\sqrt{N} \to 0$, as $N \to \infty$, for $j > j_c$. The distribution

function of the random variable $\lim_{N\to\infty} N^{-1/2} h_{[Nl/\tan\theta_c + \sqrt{N}\eta]}$ can be represented as

$$F(\rho) = \begin{cases} 0, & \text{if } \rho < 0 \\ \lim_{N\to\infty} \Pr(j_f < Nl/\tan\theta_c + \sqrt{N}\eta), & \text{for } \rho = 0 \\ \int_{-\infty}^{\rho} f(\tau)\, d\tau, & \text{if } \rho > 0 \end{cases}$$

Comparing the last expression with Eq. (3.46) one concludes that

$$\lim_{N\to\infty} \Pr[j_f \leqslant Nl/\tan\theta_c + \sqrt{N}\eta]$$
$$= \frac{1}{2}\left\{1 + \operatorname{erf}\left[\eta \tan\theta_c \sqrt{\frac{\tan\theta_c}{-2l\Phi''(i\log\xi_2)}}\right]\right\}$$

Thus

$$\lim_{N\to\infty} N^{-1/2}(j_c - Nl/\tan\theta_c)$$

has normal distribution with mean 0 and variance

$$v = -\frac{l\Phi''(i\log\xi_2)}{\tan^3\theta_c}$$

The last expression coincides with the variance announced in ref. 3.

4. SOS INTERFACE NEAR AN ATTRACTING LINE

The state space of height variables in this version of the SOS model is $\mathbf{Z}^1$. The joint distribution of the sequence of height variables $\boldsymbol{h}_{N-1} \equiv \{h_j\}_{j=1}^{N-1}$ is given by

$$\mathbf{P}(\boldsymbol{h}_{N-1}) = \Sigma_{N,L,R}^{-1} \exp\left[-\beta J \sum_{j=1}^{N} |h_j - h_{j-1}| + \beta B \sum_{j=1}^{N-1} \delta(h_j; 0)\right] \quad (4.1)$$

where $h_j \in \mathbf{Z}^1$, $\forall j$; J, $b > 0$, and $h_0 = L$, $h_N = R$ (the boundary conditions).

4.1. The Integral Representation for the Partition Function

The partition function $\Sigma_{N,L,R}$ is given by

$$\Sigma_{N,L,R} = \sum_{h_1,\ldots,h_N=-\infty}^{\infty} \exp\left[-\beta J \sum_{j=1}^{N} |h_j - h_{j-1}| + \beta b \sum_{j=1}^{N-1} \delta(h_j; 0)\right] \delta(h_N; R) \quad (4.2)$$

Analogously to the previous section introduction of a transfer operator and analysis of its spectral properties (see Appendix) yield the following expression for the partition function

$$\Sigma_{N,L,R} = \mathscr{S}_{N,L,R} + \mathscr{A}_{N,L,R} + \mathscr{D}_{N,L,R}$$

where

$$\mathscr{S}_{N,L,R} = \frac{1}{4\pi} \int_{-\pi}^{\pi} d\omega\, \Lambda^N(\omega) \left[e^{i\omega(|L|-|R|)} - \frac{(e^{i\omega}-\eta_2)(e^{i\omega}-\eta_1)}{(1-\eta_2 e^{i\omega})(1-\eta_1 e^{i\omega})} e^{i\omega(|L|+|R|)} \right]$$

is the contribution from continuous spectrum with symmetrical associated "eigenvectors,"

$$\mathscr{A}_{N,L,R} = \frac{1}{4\pi} \int_{-\pi}^{\pi} d\omega\, \Lambda^N(\omega) [e^{i\omega(L-R)} - e^{i\omega(L+R)}]$$

is the contribution from continuous spectrum with antisymmetric associated "eigenvectors" and

$$\mathscr{D}_{N,L,R} = \left[\frac{\sinh \beta J}{\cosh \beta J - \cosh(\log \eta_1)} \right]^N \left[e^{\beta b} + \frac{2}{\eta_1^2 - 1} \right]^{-1} \eta_1^{-|L|-|R|}$$

is the point spectrum contribution. Therefore, if $LR \geqslant 0$ (that is, the end points of the interface are fixed on the same side of the pinning line)

$$\Sigma_{N,L,R} = Z_{N,L,R} - \mathscr{J}_{N,L,R} + \mathscr{D}_{N,L,R}$$

where

$$\mathscr{J}_{N,L,R} = \frac{1-e^{-\beta b}}{\pi} \int_{-\pi}^{\pi} d\omega\, e^{i\omega(|L|+|R|)} \frac{\cos\omega - \cosh \beta J}{(1-\eta_2 e^{i\omega})(e^{-i\omega}-\eta_1)} \tag{4.3}$$

while

$$\Sigma_{N,L,R} = \frac{1}{2\pi} \int_{-\pi}^{\pi} d\omega\, \Lambda^N(\omega)\, e^{i\omega(|L|+|R|)} \times \frac{e^{-\beta b}(1-e^{2i\omega})}{(1-\eta_2 e^{i\omega})(1-\eta_1 e^{i\omega})} + \mathscr{D}_{N,L,R} \tag{4.4}$$

when $LR \leqslant 0$ (that is, when the end points of the interface are fixed on the different sides of the pinning line, forcing the interface to cross the pinning line). Above we used the notations

$$\eta_{1,2} = \tfrac{1}{2}a \pm \sqrt{\tfrac{1}{4}a^2 - 1 + 2e^{-\beta b}}$$

where $a = (1 - e^{-\beta b})(e^{\beta J} + e^{-\beta J})$.

In all cases the partition function (4.2) is a sum of two terms: the contribution from continuous spectrum (an integral) and the contribution from point spectrum $\mathscr{D}_{N,L,R}$. Which of the two terms gives the leading-order term in the asymptotic expansion for the partition function depends on the exact values of the parameters l, r, βJ, βb, (where l and r determine the boundary conditions via $L = [lN]$ and $R = [rN]$). We call Phase I the range of parameters where $\mathscr{D}_{N,L,R}$ dominates over the continuous spectrum contribution. The complementary region is called Phase II.

4.2. The Asymptotic Expansion for the Partition Function

Similar to the previous section the large N asymptotic expansion fat the partition partition function $\Sigma_{N,L,R}$ is derived differently depending on whether the saddle point $\omega_+^* = ig(|l| + |r|)$ of the integrands in Eqs. (4.3) and (4.4) is above or below the pole $\omega_0 = i \log \eta_1$. The condition $\omega_+^* = i \log \eta_1$ implies

$$\frac{\sqrt{1 + (|l| + |r|)^2 \sinh^2 \beta J} - (|l| + |r|) \cosh \beta J}{1 - |l| - |r|} = \eta_1$$

or

$$|l| + |r| = e^{\beta b} - 1 \equiv \tan \vartheta_c \tag{4.5}$$

If $|l| + |r| < e^{\beta b} - 1$, then the saddle point is below the pole ω_0 and the integration contour in Eqs. (4.3) and (4.4) can be deformed into the steepest descent path without crossing the pole ω_0. Using the steepest descent method, see ref. 11, one obtains

$$\Sigma_{N,L,R} = \frac{\Lambda^N(\omega_-^*) \exp[i\omega_-^*(L-R)]}{\sqrt{-2\pi N \Phi''(\omega_-^*)}} [1 + O(N^{-1})] + \mathscr{D}_{N,L,R} \tag{4.6}$$

when $lr > 0$, and

$$\Sigma_{N,L,R} = \mathscr{D}_{N,L,R}[1 + O(e^{-\varepsilon N})] \tag{4.7}$$

when $lr < 0$, where $\varepsilon \equiv \varepsilon(l, r) > 0$ as long as $|l| + |r| < e^{\beta b} - 1$.

If $|l|+|r|>e^{\beta b}-1$, then prior to application of the saddle point method the residue theorem must be applied to deform the original integration contour into the steepest descent path. Note that the residue contributions to the integrals in Eqs. (4.3) and (4.4) equal $-\mathscr{D}_{N,L,R}$. Therefore

$$\Sigma_{N,L,R}=\frac{\Lambda^N(\omega_-^*)\exp[i\omega_-^*(L-R)]}{\sqrt{-2\pi N\Phi''(\omega_-^*)}}[1+O(N^{-1})] \tag{4.8}$$

when $lr>0$, and

$$\Sigma_{N,L,R}$$
$$=\frac{e^{-\beta b}(1-e^{i2\omega_+^*})}{(1-\eta_1 e^{i\omega_+^*})(1-\eta_2 e^{i\omega_+^*})}\frac{\Lambda^N(\omega_+^*)\exp[i\omega_+^*(|L|+|R|)]}{\sqrt{-2\pi N\Phi''(\omega_+^*)}}[1+O(N^{-1})] \tag{4.9}$$

when $lr<0$.

4.3. The Distribution of the Height Variables

The distribution of the interface fluctuations can be found using the identity

$$\Pr[h_j=x]=\frac{\Sigma_{j,L,x}\Sigma_{N-j,x,R}}{\Sigma_{N,L,R}}e^{\beta b\,\delta(x;0)} \tag{4.10}$$

and Eqs. (4.6)–(4.9) in much the same way as in Section 4. In particular, the concentrating values for the random variables $h_{[\gamma N]}/N$—the equilibrium shape of the interface in the macroscopic scale—are given by

$$\chi_\gamma^*=l-\gamma(l-r),\quad \gamma\in[0;1] \qquad \text{when} \quad |l|+|r|\geqslant e^{\beta b}-1 \tag{4.11}$$

When $|l|+|r|<e^{\beta b}-1$ the equilibrium position χ_γ^* is still given by Eq. (4.11) if $l,r>0$ and $Z_{N,L,R}$ dominates over $\mathscr{D}_{N,L,R}$, that is, if the system is in Phase II. If the system is in Phase I, that is, if the main asymptotics of $\Sigma_{N,L,R}$ is given by $\mathscr{D}_{N,L,R}$ (as, e.g., in the case $r=0$, $|l|<e^{\beta b}-1$) then interface's equilibrium position is given by

$$\chi_\gamma^*=\begin{cases} l-\gamma\tan\vartheta_c, & \gamma\in[0;\,l/\tan\vartheta_c] \\ 0, & \gamma\in[l/\tan\vartheta_c;\,1-r/\tan\vartheta_c] \\ r-(1-\gamma)\tan\vartheta_c, & \gamma\in[1-r/\tan\vartheta_c;\,1] \end{cases} \tag{4.12}$$

when $l, r > 0$, and by similar expressions for other signs of l and r. Note that since $|l| + |r| < \tan \vartheta_c$ is a necessary condition for $\Sigma_{N,L,R} \sim \mathscr{D}_{N,L,R}$, the interval $[l/\tan \vartheta_c; 1 - r/\tan \vartheta_c]$ is non-empty. It is clear from Eqs. (4.10) and (4.12) that in Phase I a macroscopically large part of the interface is pinned to the line $h = 0$, while in Phase II interface is unpinned (that is $h_j = 0$ only for a few j's). The function $e^{\beta b} - 1$ is the $\tan(\cdot)$ of the contact angle—the angle between the inclined parts of the interface and the pinning line $h = 0$. The $b - T$ phase diagrams for the SOS interface (4.1) were plotted on Fig. 5.

In Phase II the fluctuations of the interface are asymptotically the same as in the case of the interface (2.1) with the identical boundary conditions and, hence, their distribution is given by Eq. (2.15). In Phase I the fluctuations of the inclined parts of the interface are qualitatively the same as the fluctuations of the inclined parts of the interface (3.1). Their distribution is given by Eq. (3.39) (with $v = -\Phi''(i \log \eta_1)$) when $\gamma \in (0, l/\tan \vartheta_c)$ and

$$\Pr[h_{[\gamma N]} = [\chi_\gamma^* N + \tau \sqrt{N}]] = \frac{1}{\sqrt{2\pi(1-\gamma)\, vN}} \exp\left(-\frac{\tau^2}{2(1-\gamma)\, v}\right) + O(N^{-1})$$

when $\gamma \in (1 - r/\tan \vartheta_c; 1)$.

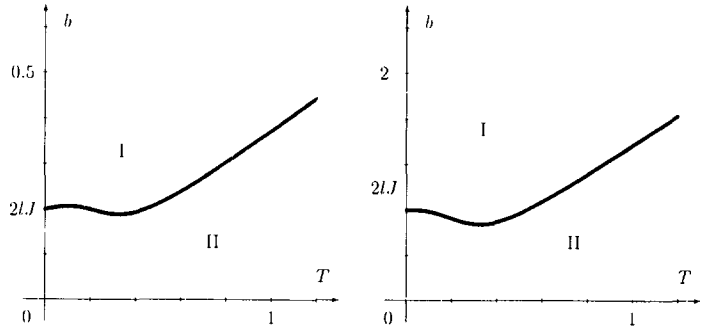

Fig. 5. The $b - T$ phase diagram for the SOS interface near a pinning line. The values of parameters are $l = 0.1, r = 0.12, J = 1$ (left) and $l = r = 0.1, J = 1$ (right). In Phase I the interface has contact with the line at a macroscopically large number of points. In Phase II the interface is the straight line joining the boundary points $L = [lN]$ and $R = [rN]$.

When $\gamma \in (l/\tan \vartheta_c; 1 - r/\tan \vartheta_c)$ a short calculation (analogous to that yielding Eq. (3.40)) yields

$$\lim_{N \to \infty} \Pr[h_{[\gamma N]} = k] = \frac{\eta_1^{-2|k|}}{e^{\beta b} + 2(\eta_1^2 - 1)^{-1}} e^{\beta b \delta(k;0)}$$

The fluctuations of the interface in the vicinity of the contact point $\gamma = l/\tan \theta_c$ can be derived in much the same way as the similar fluctuations of the interface (3.1). For $\gamma = l/\tan \vartheta_c$, $L = [lN]$, $\chi = [\rho \sqrt{N}]$, and $\rho > 0$ one obtains

$$\begin{aligned}
&\Sigma_{[\gamma N + \zeta \sqrt{N}], L, \chi} \\
&\quad = \frac{[\Lambda(i \log \eta_1)]^{[\gamma N + \zeta \sqrt{N}]} \eta_1^{-L+\chi}}{\sqrt{2\pi \gamma v N}} \left\{ \exp\left[-\frac{(\rho + \zeta \tan \vartheta_c)^2}{2\gamma v} \right] + O(N^{-1/2}) \right\} \\
&\qquad + \frac{1 - \operatorname{erf}[(\rho + \zeta \tan \vartheta_c)/\sqrt{\gamma v}]}{2} \\
&\qquad \times \frac{[\Lambda(i \log \eta_1)]^{[\gamma N + \zeta \sqrt{N}]} \eta_1^{-L-\chi}}{e^{\beta b} + 2(\eta_1^2 - 1)^{-1}} [1 + O(N^{-1/2})]
\end{aligned} \tag{4.13}$$

where $v = -\Phi''(i \log \eta_1)$, while

$$\begin{aligned}
&\Sigma_{[\gamma N + \zeta \sqrt{N}], L, \chi} \\
&\quad = \frac{[\Lambda(i \log \eta_1)]^{[\gamma N + \zeta \sqrt{N}]} \eta_1^{-L+\chi}}{2[e^{\beta b} + 2(\eta_1^2 - 1)^{-1}]} \left\{ 1 - \operatorname{erf}\left(\frac{\rho + \zeta \tan \vartheta_c}{\sqrt{\gamma v}} \right) + O(N^{-1/2}) \right\}
\end{aligned}$$

if $\rho < 0$. Also, up to an exponentially small correction

$$\Sigma_{N - [\gamma N + \zeta \sqrt{N}], \chi, R} = \frac{\eta_1^{-|\chi| - R}}{e^{\beta b} + (\eta_1^2 - 1)^{-1}} [\Lambda(i \log \eta_1)]^{N - [\gamma N + \zeta \sqrt{N}]}$$

Therefore for $\gamma = l/\tan \vartheta_c$

$$\begin{aligned}
&\Pr[h_{[\gamma N + \zeta \sqrt{N}]} = [\rho \sqrt{N}]] \\
&\quad = \frac{1}{\sqrt{2\pi \gamma v N}} \exp\left[-\frac{(\rho + \zeta \tan \vartheta_c)^2}{2\gamma v} \right] + O(N^{-1})
\end{aligned} \tag{4.14}$$

if $\rho > 0$, and

$$\Pr[h_{[\gamma Nl+\zeta\sqrt{N}]} = [\rho\sqrt{N}]] = O(\eta_1^{2\rho\sqrt{N}})$$

if $\rho < 0$.

If χ is kept fixed as $N \to \infty$ then

$$\lim_{N\to\infty} \Pr[h_{[\gamma Nl+\zeta\sqrt{N}]} = \chi] = \frac{\eta_1^{-2|\chi|}\, e^{\beta b\, \delta(\chi;\,0)}}{e^{\beta b} + (\eta_1^2 - 1)^{-1}} \frac{1 - \operatorname{erf}[(\rho + \zeta \tan \vartheta_c)/\sqrt{\gamma v}]}{2} \tag{4.15}$$

Summarizing Eqs. (4.14) and (4.15) one concludes that the random variable $\lim_{N\to\infty} N^{-1/2} h_{[\gamma N+\zeta\sqrt{N}]}$ has, an atom at the origin, and

$$\lim_{N\to\infty} \Pr\left[\frac{h_{[\gamma N+\zeta\sqrt{N}]}}{\sqrt{N}} \leqslant \rho\right] = \begin{cases} 0, & \text{if } \rho < 0 \\ \dfrac{1}{2}\left[1 + \operatorname{erf}\left(\dfrac{\rho + \zeta \tan \vartheta_c}{\sqrt{2\gamma v}}\right)\right], & \text{if } \rho \geqslant 0 \end{cases}$$

The "thin structure" of the atom is given by the distribution of the unproper random variable

$$\lim_{N\to\infty} h_{[lN/\tan\vartheta_c + \zeta\sqrt{N}]}$$

see Eq. (4.15).

5. DISCUSSION AND CONCLUDING REMARKS

5.1. Phase Diagrams at Low Temperature

Typical $b - T$ phase diagrams for the models of Sections 3 and 4 were plotted on Figs. 1, 2 and 5. As a function of temperature $T = 1/\beta$ the free energy (corresponding to the interface near an attracting wall, see Section 3)

$$f(\beta) = -\lim_{N\to\infty} \frac{1}{\beta N} \log \Theta_{N,L,R}$$

can be analytic for all $T > 0$, if the attraction of the wall, described by the parameter b, is small. It can have (only) one point of nonanalyticity, if the attraction of the wall is sufficiently strong. Finally, the free energy can have

two or even three points of nonanalyticity, if $E_N^{(u)} = J|L-R|$—the energy of the shortest interface joining the left and the right boundaries—and $E_N^{(p)} = J(L+R) - b(N-1)$—the energy of the totally pinned interface $h_j = 0$, $j = 1,..., N-1$—are approximately equal. The location of the coexistence line at $T=0$ is, of course, completely determined by the energies $E_N^{(u)}$ and $E_N^{(p)}$ and is given by $b = 2J \min(l, r)$.

The main features of the low temperature behavior of the coexistence line can be seen from the low temperature expansions for the "free energies" associated with pinned and unpinned interfaces. Consider first the case $L = R$. The "free energy" associated with a pinned interface

$$f^{(p)}(\beta) = -\frac{1}{\beta} \log \frac{\sinh \beta J}{\cosh \beta J - (\xi_2 + \xi_2^{-1})/2} - \frac{2l}{\beta} \log \xi_2$$

has the following expansion at $T=0$

$$\begin{aligned} f^{(p)}(1/T) &= 2lJ - b + T \sum_{k=1}^{\infty} \frac{e^{-2k\beta J}}{k} - T \sum_{k=1}^{\infty} \frac{e^{-2k\beta J}}{k(1-e^{-\beta b})^k} - 2lT \sum_{k=1}^{\infty} \frac{e^{-k\beta b}}{k} \\ &\approx 2lJ - b - Te^{-(2J+b)/T} - 2lTe^{-b/T} \end{aligned} \tag{5.1}$$

while the "free energy" associated with an unpinned interface

$$f^{(u)}(\beta) = -1/\beta \log \coth(\beta J/2)$$

has the low temperature expansion

$$f^{(u)}(\beta) = -2T \sum_{k=1}^{\infty} \frac{e^{-(2k-1)\beta J}}{2k-1} = -2Te^{-J/T} + O(Te^{-3J/T})$$

Therefore for small T the coexistence line $b(T)$ is given by

$$b(T) \approx 2lJ + 2T(e^{-J/T} - le^{-2lJ/T})$$

Hence, an arbitrary order derivative of $b(T)$ at $T=0$ is zero, and the coexistence line bends down for small T if $l \in (0; 1/2)$. The downward direction of the coexistence line is clearly due to the energetic cheapness of the entropy $s(E)$ associated with the partially pinned interface (that is, the small magnitude of the derivative $s'(E)$ in the vicinity of the ground state energy). Of course, the energetic cost of the entropy associated with the pinned interface itself is rather high, what is energetically cheap is the entropy associated with the inclined parts of the partially pinned interface,

which are always present if $l > 0$. Similar argument can be used to explain the low temperature behaviour of the coexistence line in the case $l \neq r$.

The low temperature behavior of the coexistence line in the case of an interface near a pinning line is the same (within the approximation in the above formulae). This is due to the fact that only unpinned parts of the interface determine the main terms of the low temperature asymptotics for $b(T) - b(0)$ (although $b(0)$ depends crucially on the pinned part of the interface but it is the same for the wall and for the line).

5.2. Interface Shape at Contact Points

Consider continuum limits

$$h(\eta) = \lim_{N \to \infty} N^{-\gamma} h_{[lN/\tan\theta_c + \eta N^\gamma]}, \quad \gamma \in [0; 1] \tag{5.2}$$

where $\eta \in (-\infty, \infty)$ for $\gamma \in [0, 1)$, and $\eta \in [-l/\tan\theta_c; 1 - l/\tan\theta_c]$ for $\gamma = 1$. Section 4 contains comprehensive description of the continuum limit (5.2) for the case $\gamma = 1$ (macroscopic scale), see Eq. (3.36). In a similar way it is possible to investigate the continuum limit (5.2) for $\gamma \in [0; 1)$. It is sufficient to consider only the boundary conditions $L = [lN]$, $l \neq 0$, and $R = 0$. Below we describe the results of the investigation.

For $\gamma \in (1/2; 1)$ the typical interfaces $\{h_j\}_{j=1}^N$ merge in the continuum limit (5.2) into the function

$$h(\eta) = \begin{cases} -\eta \tan\theta_c, & \eta \in (-\infty, 0) \\ 0, & \eta \in [0; \infty) \end{cases} \tag{5.3}$$

Therefore in the scales corresponding to $\gamma \in (1/2, 1)$ the interface (3.1) is deterministic (does not fluctuate), and it has a cusp at the first-contact point.

For $\gamma = 1/2$ the interface fluctuations do not vanish as $N \to \infty$, as a consequence the limit (5.2) exists only in distribution. This limit is a random function

$$h^{(\kappa)}(\eta) = \begin{cases} (\kappa - \eta)\tan\theta_c, & \eta \in (-\infty, \kappa) \\ 0, & \eta \in [\kappa, \infty) \end{cases}$$

where κ is a normally distributed random variable with mean 0 and variance $v = -l\Phi''(i \log \xi_2)/\tan^3\theta_c$. Note that the fluctuations do not affect the shape of the functions $h^{(\kappa)}(\eta)$. The only effect of fluctuations is a random shift of $h^{(0)}(\eta)$ along the horizontal axis, while the shape of the interface remains the same as in the case $\gamma \in (1/2, 1)$.

For $\gamma \in (0, 1/2)$ the limit (5.2) does not exists as a proper random variable, since the fluctuations of $N^{-\gamma} h_{[lN/\tan\theta_c + \eta N^\gamma]}$ grow unboundedly as $N \to \infty$ in that case. However, if we are interested only in the shape of the interface, and the interface location is irrelevant to us, it is reasonable to consider the continuum limits

$$s(\eta) = \lim_{N \to \infty} N^{-\gamma} h_{[j_c + \eta N^\gamma]}, \quad \gamma \in [0, 1/2] \tag{5.4}$$

where j_c is the point of first contact of the interface with the wall. The continuum limits (5.4) exist for all $\gamma \in (0; 1/2]$ and coincide with Eq. (5.3). That is, the *shape* of the interface in the scales corresponding to $\gamma \in (0, 1/2]$ is the same as in the case $\gamma \in (1/2; 1)$, in spite of the fluctuations.

Finally, if $\gamma = 0$ then the limit (5.4) exists only in distribution and $\{s(j)\}_{j=-\infty}^{\infty}$ is a microscopic scale trajectory of a random walk. Therefore the interface is, in some sense, shapeless when $\gamma = 0$.

Conceptually the most important conclusion of the above discussion is that the interface has a cusp at a first-contact point in all scales except microscopic (where the interface is shapeless). Contrary to the opinions which can be often found in physics literature interface rounding does not take place in any scale.

APPENDIX. SPECTRAL PROPERTIES OF THE MATRICES $\hat{\Pi}_k$

The $(2k+1) \times (2k+1)$ matrices $\hat{\Pi}_k$, $k = 1, 2, \ldots$; are given by

$$\hat{\Pi}_k = \{ e^{-\beta J |j-l| + \beta b [\delta(j;0) + \delta(l;0)]/2} \}_{j,l=-k}^{k}$$

To solve the spectral problem for the matrices $\hat{\Pi}_k$ we first solve the spectral problem for the inverse matrix $\hat{\Pi}_k^{-1}$ and use the facts that the matrices $\hat{\Pi}_k$ and $\hat{\Pi}_k^{-1}$ have a common set of eigenvectors and if $\lambda \neq 0$ is an eigenvalue of $\hat{\Pi}_k^{-1}$ then λ^{-1} is an eigenvalue of $\hat{\Pi}_k$.

One can represent $\hat{\Pi}_k$ as the following product

$$\hat{\Pi}_k = \hat{D}_k \hat{L}_k \hat{D}_k \tag{A1}$$

where

$$\hat{D}_k = \{ e^{\beta b \, \delta(j;0)/2} \, \delta(j;l) \}_{j,l=-k}^{k}$$

are diagonal matrices, and

$$\hat{L}_k = \{ e^{-\beta J |j-l|} \}_{j,l=-k}^{k}$$

The matrices $\hat{D}_k^{-1}$ are given by

$$\hat{D}_k^{-1} = \{e^{-\beta b\,\delta(j;\,0)/2}\,\delta(j;\,l)\}_{j,\,l=-k}^{k}$$

The matrices $\hat{L}_k^{-1}$ are given by

$$\hat{L}_k^{-1} = \coth \beta J \hat{E}_k - \frac{1}{2 \sinh \beta J}\,\hat{M}_k$$

where $\hat{E}_k$ is the $(2k+1)\times(2k+1)$ identity matrix and $\hat{M}_k$ is given by

$$\hat{M}_k \equiv \{\mu_{j,\,l}\}_{j,\,l=-k}^{k} = \begin{pmatrix} e^{-\beta J} & 1 & & & & & & \\ 1 & 0 & 1 & & & & & \\ & 1 & 0 & & & & & \\ & & & \ddots & & & & \\ & & & & 0 & 1 & & \\ & & & & 1 & 0 & 1 & \\ & & & & & 1 & e^{-\beta J} \end{pmatrix}$$

Therefore

$$\hat{\Pi}_k^{-1} = \coth \beta J \hat{E}_k - \frac{1}{2 \sinh \beta J}\,\hat{B}_k \tag{A2}$$

where

$$\hat{B}_k = \begin{pmatrix} e^{-\beta J} & 1 & & & & & & & & & \\ 1 & 0 & & & & & & & & & \\ & & \ddots & & & & & & & & \\ & & & 0 & 1 & & & & & & \\ & & & 1 & 0 & e^{-\beta b/2} & & & & & \\ & & & & e^{-\beta b/2} & a & e^{-\beta b/2} & & & & \\ & & & & & e^{-\beta b/2} & 0 & 1 & & & \\ & & & & & & 1 & 0 & & & \\ & & & & & & & & \ddots & & \\ & & & & & & & & & 0 & 1 \\ & & & & & & & & & 1 & e^{-\beta J} \end{pmatrix}$$

and $a = (1 - e^{-\beta b})(e^{\beta J} + e^{-\beta J})$.

On introduction of a new vector $\chi \equiv \{\chi_l\}_{l=-k}^{k}$ such that

$$\chi_l = e^{-\beta b\,\delta(l;\,0)}\psi_l, \quad l = -k, \ldots, k$$

the equation $\hat{B}_k \psi = \lambda \psi$, where $\psi = \{\psi_l\}_{l=-k}^{k}$, simplifies to

$$\begin{aligned} \chi_{-k} e^{-\beta J} + \chi_{-k+1} &= \lambda \chi_{-k} \\ \chi_l + \chi_{l+2} &= \lambda \chi_{l+1}, \quad l = -k, -k+1, \ldots, -2 \\ \chi_{-1} + \chi_1 &= (\lambda - a)\, e^{\beta b} \chi_0 \\ \chi_{l-2} + \chi_l &= \lambda \chi_{l-1}, \quad l = 2, 3, \ldots, k \\ \chi_{k-1} + \chi_k e^{-\beta J} &= \lambda \chi_k \end{aligned} \tag{A3}$$

When $\lambda \neq \pm 2$ the solution of (A3) with the initial condition χ_{-k}, χ_{-k+1} is given by

$$\begin{aligned} \chi_{-k+l} &= \frac{1}{x_1 - x_2} [(x_1 \chi_{-k} - \chi_{-k+1})\, x_2^l + (\chi_{-k+1} - x_2 \chi_{-k})\, x_1^l], \quad l = 0, 1, \ldots, k \\ \chi_1 &= (\lambda - a)\, e^{\beta b} \chi_0 - \chi_{-1} \\ \chi_l &= \frac{1}{x_1 - x_2} [(x_1 \chi_0 - \chi_1)\, x_2^l + (\chi_1 - x_2 \chi_0)\, x_1^l], \quad l = 2, 3, \ldots, k \end{aligned} \tag{A4}$$

where

$$x_{1,2} = \tfrac{1}{2}\lambda \pm \sqrt{\tfrac{1}{4}\lambda^2 - 1} \tag{A5}$$

(note that $x_1 + x_2 = \lambda$, $x_1 x_2 = 1$). The first equation in (A3) allows one to exclude χ_{-k+1} and to transform the first equation in (A4) to

$$\chi_{-k+l} = \frac{\chi_{-k}}{x_1 - x_2} [(e^{-\beta J} - x_2)\, x_2^l + (x_1 - e^{-\beta J})\, x_1^l], \qquad l = 0, 1, \ldots, k \tag{A6}$$

On substituting χ_0 and χ_{-1} given by Eq. (A6) in the second equation in (A4) and on substituting the expressions for χ_0 and χ_1 in the last equation in (A4) one obtains

$$\chi_l = \frac{\chi_{-k}}{(x_1 - x_2)^2} (A x_2^l + B x_1^l), \qquad l = 2, 3, \ldots, k \tag{A7}$$

where

$$\begin{aligned} A &= (e^{-\beta J} - x_2)[2x_1 - e^{\beta b}(\lambda - a)]\, x_2^k + (x_1 - e^{-\beta J})[\lambda - e^{\beta b}(\lambda - a)]\, x_1^k \\ B &= (e^{-\beta J} - x_2)[e^{\beta b}(\lambda - a) - \lambda]\, x_2^k + (x_1 - e^{-\beta J})[e^{\beta b}(\lambda - a) - 2x_2]\, x_1^k \end{aligned}$$

The last equation in (A3) and Eq. (A7) yield the equation for the eigenvalues $\{\lambda_j\}_{j=1}^{2k+1}$ of the matrix $\hat{B}_k$ which can be factorized as

$$\{x_1^{2k}(x_1 - e^{-\beta J})[2x_2 - e^{\beta b}(\lambda - a)] + (e^{-\beta J} - x_2)[2x_1 - e^{\beta b}(\lambda - a)]\}$$
$$\times [(e^{-\beta J} - x_2)\, x_2^{2k} + (x_1 - e^{-\beta J})] = 0$$

Therefore the problem of finding the eigenvalues of the matrix $\hat{B}_k$ reduces to solution of the following two equations

$$x^{2k+1} = \frac{1 - xe^{-\beta J}}{x - e^{-\beta J}} \tag{A8}$$

$$x^{2k+1} = \frac{1 - xe^{-\beta J}}{x - e^{-\beta J}} \frac{1 - x\eta_1}{x - \eta_1} \frac{1 - x\eta_2}{x - \eta_2} \tag{A9}$$

where

$$\eta_{1,2} = \tfrac{1}{2}a \pm \sqrt{\tfrac{1}{4}a^2 - 1 + 2e^{-\beta b}}$$

Note that for $\beta J > 0$, $\beta b > 0$ one has

$$1 < \eta_1 < e^{\beta J}, \quad -1 < \eta_2 < e^{-\beta J}$$

and $\eta_2 \in (0; e^{-\beta J})$ if $e^{-\beta b} \in (0; 1/2)$.

Usually the equations of the type (A8) and (A9) are investigated using the so-called graphical analysis which would yield the following results. The $2k+2$ solutions $\{\xi_j = e^{i\varphi_j}\}_{j=1}^{2k+2}$ of the equation (A8) and the $2k+2$ solutions $\{\zeta_j\}_{j=1}^{2k+2}$, of the equation (A9) satisfying $|\zeta_j| = 1$ are distributed on the unit circle uniformly enough to assure that

$$\frac{1}{2k+2} \sum_{j=1}^{2k+2} [f(\xi_j) + f(\zeta_j)] \to \frac{1}{\pi} \int_{-\pi}^{\pi} f(e^{i\omega}) d\omega \tag{A10}$$

as $k \to \infty$, for any function $f(z)$ continuous on the unit circle $|z| = 1$.

Although the graphical analysis of Eq. (A8) is very simple the (careful) graphical analysis of Eq. (A9) is rather cumbersome. It turns out that it is possible to obtain an asymptotic estimate for the sum in the l.h.s. of Eq. (A10) (and, in fact, a much sharper one than that given by Eq. (A10)) without using the graphical analysis at all. We explain the main steps of the alternative method below.

First we give a rough description of the location of the roots of the equations (A8) and (A9). The proof of the next lemma is omitted. It is not

entirely trivial, but rather lengthy, and can be found in the complete version of this paper.[11]

Lemma A1. The equation (A8) has $2k+2$ solutions $\{\xi_l\}_{l=1}^{2k+2}$ satisfying $|\xi_l|=1$, $l=1, 2,..., 2k+2$. The equation (A9) has $2k+4$ solutions $\{\zeta_l\}_{l=1}^{2k+4}$ such that $|\zeta_l|=1$, $l\neq k+1, k+3$ and

$$\zeta_{k+1}=\zeta_{k+3}^{-1}=\zeta_* \in (\eta_1^{-1}; 1)$$

if

$$e^{\beta b}-1>\frac{2}{(e^{\beta J}-1)[k(1-e^{-\beta J})+1]} \tag{A11}$$

and $|\zeta_{k+1}|=|\zeta_{k+3}|=1$ if

$$e^{\beta b}-1\leqslant\frac{2}{(e^{\beta J}-1)[k(1-e^{-\beta J})+1]} \tag{A12}$$

∎

Now it is possible to describe the eigenvalues $\{\lambda_j\}_{j=1}^{2k+1}$ of the matrix $\hat{B}_k$ in terms of the solutions $\{\xi_l\}_{l=1}^{2k+2}$ and $\{\zeta_l\}_{l=1}^{2k+4}$ of the equations (A8) and (A9), respectively. We assume that the solutions $\{\xi_l=e^{i\varphi_l}\}_{l=1}^{2k+2}$, $\varphi_l\in(-\pi;\pi]$ are ordered according to the principal values of their arguments, that is,

$$-\pi<\varphi_1\leqslant\varphi_2\leqslant\cdots\leqslant\varphi_{2k+2}\leqslant\pi$$

Analogously, we assume that the solutions $\{\varphi_l\}_{l=1}^{2k+4}$ are ordered according to the principal values of their arguments, and the solutions having identical arguments (like the possible real positive solutions) are ordered according to their absolute values.

Note that the points $\xi=\pm1$ and $\zeta=\pm1$ are always solutions, and any solution $\xi\neq1$ or $\zeta\neq1$ has a pair ξ^{-1} or ζ^{-1}, respectively. Therefore

$$\xi_{2k+2}=-1,\quad \xi_{k+2}=1,\qquad \text{and}\qquad \xi_l=\xi_{2k+2-l}^{-1},\quad l=1, 2,..., k$$

Analogously,

$$\zeta_{2k+4}=-1,\quad \zeta_{k+2}=1,\qquad \text{and}\qquad \zeta_l=\zeta_{2k+4-l}^{-1},\quad l=1, 2,..., k+1$$

Investigation of Eq. (A3) shows that the solutions $\xi=-1$, $\zeta=-1$ are spurious, that is, $\lambda=-2$ is not an eigenvalue of the matrix $\hat{B}_k$. These solutions appeared as a result of algebraic manipulations (namely, multiplication

of the equation $\chi_{k-1} = (\lambda - e^{-\beta J})\,\lambda_k$ by $(x_1 - x_2)^2$, which is a multiplication by zero when $x_2 = \pm 1$). The solutions $\xi = 1, \zeta = 1$ are spurious as well unless

$$e^{\beta b} - 1 = \frac{2}{(e^{\beta J} - 1)[k(1 - e^{-\beta J}) + 1]}$$

when $\zeta = 1$ is a triple zero, that is, $\zeta_{k+1} = \zeta_{k+2} = \zeta_{k+3} = 1$.

Each pair $\xi_l, \xi_{2k+2-l} (= \xi_l^{-1})$, $l = 1,..., k$ and $\zeta_l, \zeta_{2k+4-l} (= \zeta_l^{-1})$, $l = 1,..., k+1$ give rise only to a single eigenvalue λ and a single eigenfunction ψ associated with λ. Therefore, according to Eq. (A5) the eigenvalues $\{\lambda_j\}_{j=1}^{2k+1}$ are given by

$$\lambda_j = \begin{cases} \xi_j + \xi_{2k+2-j}, & j = 1, 2,..., k \\ \zeta_{j-k} + \zeta_{2k+4-(j-k)}, & j = k+1, k+2,..., 2k+1 \end{cases} \tag{A13}$$

To find the eigenvectors associated with the eigenvalues $\{\lambda_j\}_{j=1}^{2k+2}$ note that if x_2 satisfy Eq. (A8) then Eq. (A7) can be rewritten as

$$\chi_{k-l} = -\frac{\chi_{-k}}{x_1 - x_2}\,[(e^{-\beta J} - x_2)\,x_2^l + (x_1 - e^{-\beta J})\,x_1^l], \qquad l = 0, 1,..., k-2$$

that is, $\chi_{k-l} = -\chi_{-k+l}$, $l = 0, 1,..., k-2$, due to Eq. (A6). Moreover, if x_2 is a solution of the equation (A8) then Eq. (A6) yields $\chi_0 = 0$ and, hence, the second equation in (A4) yields $\chi_1 = -\chi_{-1}$. Therefore, the eigenvectors associated with the eigenvalues $\{\lambda_j = \xi_j + \xi_j^{-1}\}_{j=1}^{k}$ are antisymmetric and are given by $\{\chi_{j,l}\}_{l=-k}^{k}$, $j = 1, 2,..., k$; where

$$\chi_{j,l} = \frac{\chi_{-k}}{\xi_j^{-1} - \xi_j}\,[(e^{-\beta J} - \xi_j)\,\xi_j^{l+k} + (\xi_j^{-1} - e^{-\beta J})\,\xi_j^{-l-k}],$$

$$l = -k, -k+1,..., -1$$

$\chi_{j,0} = 0$, and $\chi_{j,l} = -\chi_{j,-l}$, $l = 1, 2,..., k$.

A short calculation shows that

$$\sum_{l=1}^{k} |\chi_{j,l}|^2 = \frac{|\chi_{-k}|^2}{|\xi_j^{-1} - \xi_j|^2}\left[4ke^{-\beta J}\left(\cosh \beta J - \frac{1}{2}\lambda_j\right) + 2 - e^{-\beta J}\lambda_j\right]$$

where we used Eq. (A8) to get rid of high powers of ξ_j. Thus the orthonormal (real) eigenvectors of the matrix $\hat{B}_k$ associated with the eigenvalues $\{\lambda_j\}_{j=1}^{k}$ are given by

$$\psi_j = \left\{ \psi_{j,l} \equiv \sqrt{\frac{\cosh \beta J - (1/2)\,\lambda_j}{4k(\cosh \beta J - (1/2)\,\lambda_j) + e^{\beta J} - (1/2)\,\lambda_j}} (\xi_j^l - \xi_j^{-l}) \right\}_{l=-k}^{k}$$

$$= \left\{ \psi_{j,l} \equiv \frac{\sin l\varphi_j}{\sqrt{k}} [1 + O(k^{-1})] \right\}_{l=-k}^{k}$$

Consider now the eigenvalues $\{\lambda_j = \zeta_{j-k} + \zeta_{j-k}^{-1}\}_{j=k+1}^{2k+1}$, where ζ_l are solutions of the equation (A9). Note that if x_2 is a solution of the equation (A9) then Eq. (A7) can be rewritten as

$$\chi_{k-l} = \frac{\chi_{-k}}{x_1 - x_2} [(e^{-\beta J} - x_2)\, x_2^l + (x_1 - e^{-\beta J})\, x_1^l], \quad l = 0, 1, \ldots, k-2$$

that is, $\chi_{k-l} = \chi_{-k+l}$, $l = 0, 1, \ldots, k-2$; due to Eq. (A6). Moreover, if x_2 is a solution of the equation (A9) then Eq. (A6) yields $(\lambda - a)\, e^{\beta b} \chi_0 = 2\chi_{-1}$ and, hence, the second equation in (A4) yields $\chi_1 = \chi_{-1}$. Therefore, the eigenvectors associated with the eigenvalues $\{\lambda_j\}_{j=k+1}^{2k+1}$ are symmetric and are given by

$$\left\{ \chi_{j,l} = \frac{\chi_{-k}}{\zeta_{j-k}^{-1} - \zeta_{j-k}} [(e^{-\beta J} - \zeta_{j-k})\, \zeta_{j-k}^{k-|l|} + (\zeta_{j-k}^{-1} - e^{-\beta J})\, \zeta_{j-k}^{|l|-k}] \right\}_{l=-k}^{k}$$

$j = k+1, k+2, \ldots, 2k+1$.

Since $\zeta_{k+1} \in (\eta^{-1}; 1)$ (for any $\beta b > 0$, $\beta J > 0$ if k is large enough) one has

$$\sum_{l=-k}^{k} |\chi_{k+1,l}|^2$$

$$= \frac{|\zeta_{-k}|^2}{|\zeta_{k+1}^{-1} - \zeta_{k+1}^{-1}|^2} \left\{ \zeta_{k+1}^{-2k} (\zeta_{k+1}^{-1} - e^{-\beta J})^2 \left[e^{\beta b} + \frac{2}{\zeta_{k+1}^{-2} - 1} \right] + O(k) \right\}$$

where the $O(k)$ estimate is uniform over l. Therefore the normalized eigenvector ψ_{k+1} is given by

$$\psi_{k+1} = \left\{ \psi_{k+1,l} = \zeta_{k+1}^{|l|} e^{\beta b\, \delta(l;0)/2} \left[e^{\beta b} + \frac{2}{\zeta_{k+1}^{-2} - 1} \right]^{-1/2} + O(\zeta_{k+1}^{k}) \right\}_{l=-k}^{k}$$

The solutions $\{\zeta_j\}_{j=1}^{k}$ belong to the unit circle $|\zeta| = 1$. A short calculation shows that

$$\sum_{l=-k}^{k} |\chi_{j,l}|^2 = \frac{|\chi_{-k}|^2}{|\zeta_{j-k}^{-1} - \zeta_{j-k}|^2}\left[8ke^{-\beta J}\left(\cosh \beta J - \frac{1}{2}\lambda_j\right) + O(1)\right],$$
$$j = k+1, k+2, \ldots, 2k$$

where the $O(1)$ estimate is uniform over j since ζ_{j-k} is a solution of the equation (A9). Therefore the (real) orthonormal eigenvectors ψ_j associated with the eigenvalues λ_j, $j = k+1, k+2, \ldots, 2k$; are given by

$$\psi_j = \left\{\psi_{j,l} = \frac{e^{\beta b\, \delta(l;\,0)/2}}{2i\sqrt{k}}\left[\zeta_{j-k}^{|l|} Z_j - \zeta_{j-k}^{-|l|} Z_j^{-1}\right]\left[1 + O(k^{-1})\right]\right\}_{l=-k}^{k}$$

where

$$Z_j = \sqrt{\frac{(\zeta_j - \eta_2)(\zeta_j - \eta_1)}{(1 - \zeta_j\eta_2)(1 - \zeta_j\eta_1)}}$$

Now we are ready to prove a stronger version of the estimate (A10).

Lemma A2. Let $f(z) = \sum_{l=-\infty}^{\infty} a_l z^l$ be an analytic function on a ring-shaped region $(R+\delta)^{-1} < |z| < R + \delta$, where $R > 1$, $\delta > 0$. Let $\{\xi_l\}_{l=1}^{2k+2}$ be the solutions of the equation (A8), and let $\{\zeta_l\}_{l=1}^{2k+2}$ be the solutions of the equation (A9) satisfying $|\zeta_l| = 1$, $l = 1, 2, \ldots, 2k+2$. Then

$$\frac{1}{2k+2}\sum_{l=1}^{2k+2} f(\xi_l) = a_0 + \frac{1}{2k+2}\tilde{f}(e^{-\beta J}) + O(R^{-2k}) \tag{A14}$$

and

$$\frac{1}{2k+2}\sum_{l=1}^{2k+2} f(\zeta_l) = a_0 + \frac{1}{2k+2}\left[\tilde{f}(e^{-\beta J}) + \tilde{f}(\eta_1) - \tilde{f}(\eta_1^{-1})\right] + O\left[\min(R, \eta_1)^{-2k}\right] \tag{A15}$$

where the function $\tilde{f}(z) = \sum_{l=1}^{\infty}(a_l + a_{-l})\, z^l$ is analytic on $|z| < R + \delta$.

Proof. We prove only Eq. (A15) the proof of Eq. (A14) is analogous. Since

$$\frac{1}{2k+2}\sum_{l=1}^{2k+2} f(\zeta_l) = \sum_{n=-\infty}^{\infty} a_n \frac{1}{2k+2}\sum_{l=1}^{2k+2} \zeta_l^n$$

our strategy is to obtain explicit expressions for $\sum_{l=1}^{2k+2} \zeta_l^n$ using the relations

$$s_m + A_{k-1}s_{m-1} + A_{k-2}s_{m-2} + \cdots + A_{k-m+1}s_1 + mA_{k-m} = 0, \qquad m = 1, 2, \ldots, k \tag{A16}$$

connecting coefficients of the algebraic equation

$$z^k + A_{k-1}z^{k-1} + A_{k-2}z^{k-2} + \cdots + A_0 = 0$$

with the sums of powers $s_m = \sum_{l=1}^{k} z_l^m$ of the solutions $\{z_l\}_{l=1}^{k}$ of this equation.

The relations (A16) applied to the equation

$$x^{2k+4} - A_1 x^{2k+3} + A_2 x^{2k+2} - A_3 x^{2k+1} + A_3 x^3 - A_2 x^2 + A_1 x - 1 = 0 \tag{A17}$$

yield

$$\sum_{l=1}^{2k+4} \zeta_l^n = e^{-n\beta J} + \eta_1^n + \eta_2^n, \qquad n = 1, 2, \ldots, 2k$$

Since for any solution ζ of the equation (A17) the point ζ^{-1} is a solution as well, one has

$$\sum_{l=1}^{2k+4} \zeta_l^n = e^{-|n|\beta J} + \eta_1^n + \eta_2^n, \qquad n = 1, 2, \ldots, 2k$$

Taking into account

$$\zeta_{2k+3} = \eta_1^{-1} + O(\eta_1^{-2k}) \qquad \text{and} \qquad \zeta_{2k+4} = \eta_1 + O(\eta_1^{-2k})$$

one obtains

$$\sum_{l=1}^{2k+2} \zeta_l^n = e^{-|n|\beta J} + \eta_1^{|n|} - \eta_1^{|n|} + O(\eta_1^{-2k}), \qquad n = \pm 1, \pm 2, \ldots, \pm 2k$$

The Cauchy inequalities for the coefficients of the Laurent expansion of the function $f(z)$

$$|a_n| \leqslant m(R)\, R^n, \quad n = -1, -2, \ldots \qquad \text{and} \qquad |a_n| \leqslant M(R)\, R^{-n}, \quad n = 1, 2, \ldots$$

where

$$m(R) = \max_{|z| = 1/R} f(z), \quad M(R) = \max_{|z| = R} f(z)$$

yield

$$\left| \sum_{n=-\infty}^{-2k-1} a_n \frac{1}{2k+2} \sum_{l=1}^{2k+2} \zeta_l^n \right| \leqslant \sum_{n=-\infty}^{-2k-1} m(R)\, R^n = m(R) \frac{R^{-2k}}{R-1}$$

$$\left| \sum_{n=2k+1}^{\infty} a_n \frac{1}{2k+2} \sum_{l=1}^{2k+2} \zeta_l^n \right| \leqslant \sum_{n=2k+1}^{\infty} M(R)\, R^{-n} = M(R) \frac{R^{-2k}}{R-1}$$

and

$$\left| \sum_{n=2k+1}^{\infty} (a_{-l} + a_l)\, \alpha^{-n} \right| \leqslant [m(R) + M(R)] \frac{(R\alpha)^{-2k}}{R\alpha - 1}$$

if $R\alpha > 1$. Therefore

$$\begin{aligned} &\frac{1}{2k+2} \sum_{l=1}^{2k+2} f(\zeta_l) \\ &\quad = a_0 + \frac{1}{2k+2} \sum_{l=1}^{\infty} (a_{-l} + a_l)(e^{-l\beta J} + \eta_2^l - \eta_1^{-l}) + O[\min(R, \eta_1)^{-2k}] \\ &\quad = a_0 + \frac{1}{2k+2} [\tilde{f}(e^{-\beta J}) + \tilde{f}(\eta_1) - \tilde{f}(\eta_1^{-1})] + O[\min(R, \eta_1)^{-2k}] \end{aligned}$$

as asserted. ∎

ACKNOWLEDGMENTS

The author would like to thank Jean Ruiz, for introduction to the subject of the paper, and Denjoe O'Connor, for reading the manuscript and useful comments. Some of the topics of the paper were inspired by discussions with Professor C. Pfister and Dr. Paul Upton.

REFERENCES

1. D. B. Abraham, Solvable Model with a Roughening Transition for a Planar Ising Ferromagnet, *Phys. Rev. Lett.* **44**:1165–1168 (1980).
2. D. B. Abraham and L-F. Ko, Exact Derivation of the Modified Young Equation for Partial Wetting, *Phys. Rev. Lett.* **63**:275–278 (1989).

3. D. B. Abraham, F. Latrémolière, and P. J. Upton, Divergence of the Point Tension at Wetting, *Phys. Rev. Lett.* **71**:404–407 (1993).
4. D. B. Abraham and E. R. Smith, An Exactly Solved Model with a Wetting Transition, *J. Stat. Phys.* **43**:621–643 (1986).
5. J. T. Chalker, The Pinning of a Domain Wall by Weakened Bonds in Two Dimensions, *J. Phys. A: Math. Gen.* **14**:2431–2440 (1981).
6. S. T. Chui and J. D. Weeks, Pinning and Roughening of One-Dimensional Models of Interfaces and Steps, *Phys. Rev. B* **23**:2438–2441 (1981).
7. J. De Coninck and F. Dunlop, Partial to Complete Wetting: A Microscopic Derivation of the Young Relation, *J. Stat. Phys.* **47**:827–849 (1987).
8. J. De Coninck, F. Dunlop, and V. Rivasseau, On the Microscopic Validity of the Wulff Construction and on the Generalized Young Equation, *Common. Math. Phys.* **121**:401–419 (1989).
9. J. De Coninck and J. Ruiz, Fluctuation of Interfaces and Anisotropy. *J. Phys. A: Math. Gen.* **21**:L147–L153 (1988).
10. S. Miracle-Sole and J. Ruiz, On the Wulff Construction as a Problem of Equivalence of Statistical Ensembles. In: *On Three Levels: Micro-, Meso-, and Macro-Approaches in Physics* (New York: Plenum Press, 1994, pp. 295–302).
11. A. E. Patrick, The Influence of Boundary Conditions on Solid-On-Solid Models, Dublin Insitute for Advanced Studies, Preprint DIAS-STP-96-02, (1996).
12. H. N. V. Temperley, Statistical Mechanics and the Partition of Numbers II. The Form of Crystal Surfaces, *Proc. Camb. Phil. Soc.* **48**:683–697 (1952).
13. H. N. V. Temperley, Combinatorial Problems Suggested by the Statistical Mechanics of Domains and of Rubber-Like Molecules, *Phys. Rev.* **103**:1–16 (1956).